



**Abbreviations used**

AGEs:	Advanced glycation end products
BLG:	$\beta$ -lactoglobulin
BMI:	Body mass index
BSA:	Bovine serum albumin
CEL:	Ne-(1-carboxyethyl) lysine
CFSE:	Carboxyfluorescein succinimidyl ester
CML:	Ne-(carboxymethyl) lysine
DAPI:	4'6-diamidino-2-phenylindole dihydrochloride
DCFH-DA:	7'-dichlorofluorescein diacetate
FA:	Food allergy
FD-4:	4000 d FITC-labeled dextran
FITC:	Fluorescein isothiocyanate
HC:	Healthy control
LPS:	Lipopolysaccharide
MG-H1:	N $\delta$ -(5-hydro-5 methyl-4-imidazolone-2-yl)-ornithine
NF- $\kappa$ B:	Nuclear factor- $\kappa$ B
OCR:	Oxygen consumption rate
OVA:	Ovalbumin
PI:	Propidium iodide
RAGE:	Receptor for advanced glycation end products
ROS:	Reactive oxygen species
sAF:	Skin autofluorescence
TEER:	Transepithelial electrical resistance
TJ:	Tight junction
TSLP:	Thymic stromal lymphopoietin
UPF:	Ultra-processed food
ZO-1:	Zonula occludens-1

AGEs exerted a wide range of detrimental actions on immune tolerance mechanisms. In addition, we found higher intake of dietary AGEs and accumulation of AGEs in the skin in children with FA. Altogether, these data suggest the importance of limiting exposure to dietary AGEs in children as a potential preventive strategy against FA.

**METHODS****Study design**

The potential role of AGEs in facilitating the occurrence of FA was evaluated through *in vitro* and clinical investigations. In the *in vitro* studies, we focused on the direct effects elicited by AGEs on human cells. Human enterocytes, human small intestine organ culture, and PBMCs collected from children at risk for allergy were used to investigate the effect of AGEs on gut barrier integrity, inflammation, immune response, and mitochondrial function. The clinical investigations were focused on the comparative evaluation of the intake of dietary AGEs and accumulation of AGEs in the skin in children with FA and in age-matched healthy controls (HCs).

**In vitro studies**

For all *in vitro* experiments we used a commercially available AGE-bovine serum albumin (BSA) (#ab51995, Abcam, Cambridge, UK; purity: >98%; endotoxin level: <0.100 EU/ $\mu$ g), produced by the reaction of BSA with glycolaldehyde/glyoxal. AGE-BSA was desalted with Econo-Pac chromatography columns (Bio-Rad, Milan, Italy), eluted with 0.5% (vol/vol) formic acid, and lyophilized. This molecule has been

previously used in studies on human enterocytes and PBMCs,<sup>18-22</sup> it is representative of glycated dietary proteins,<sup>18,19,23-35</sup> and the biological effects are similar to those elicited by other dietary glycated proteins.<sup>36-38</sup> All the experiments were performed in triplicate and repeated 3 times.

**Simulated infant gastrointestinal digestion**

An aliquot of AGE-BSA (6 mg) was subjected to an *in vitro* simulated gastroduodenal digestion substantially adapting the protocol of a physiologically relevant infant static model.<sup>39</sup> Considering the absence of starchy components, the oral phase of digestion was omitted. Briefly, AGE-BSA (6 mg) was suspended in 0.4 mL of simulated gastric fluid, which was 100 mM sodium chloride, 15 mM potassium chloride, and pH 5 adjusted with 1N hydrochloric acid. Gastric phase of digestion was carried out with 110 U/mL pepsin at 37°C under gentle stirring. The gastric digestion was stopped after 60 minutes by increasing the pH at 7 with 1N sodium hydroxide. To mimic the duodenal phase of digestion, the volume of gastric digests was doubled with simulated intestinal fluid (150 mM of sodium chloride, 10 mM of potassium chloride, and 85 mM of sodium bicarbonate, pH 7), and the pH was adjusted to 6.6. Duodenal digestion was simulated with pancreatin (Merck-Sigma, Milan, Italy) added up to 15 U/mL trypsin activity, omitting bile salts. A digestion of 6 mg of BSA (purchased from Sigma-Aldrich, St. Louis, Mo) and a control incubation of digestive enzymes without any protein substrate included were carried out in parallel. Immediately after 60 minutes of simulated duodenal digestion at 37°C, the digests were purified using reversed-phase Sep-pak C18 cartridges (Waters, Milford, Mass), eluting with 70% acetonitrile/0.1% (vol/vol) trifluoroacetic acid. Purified (poly)peptides were finally vacuum dried and lyophilized. The purification steps were carried out with toxin-free disposable devices. To limit the bias potentially induced by lipopolysaccharide (LPS) contamination, we assessed the LPS content as previously described.<sup>40</sup> To remove traces of LPS contamination, a 2-phase detergent-based (Triton X-114; Sigma-Aldrich) extraction was also performed, as previously described.<sup>39</sup>

**LC-MS/MS**

Aliquots of the gastroduodenal peptide digests were used for LC-MS/MS analysis using a nanoflow HPLC UltiMate 3000 coupled to a Q Exactive Orbitrap mass spectrometer (Thermo Fisher Scientific, Waltham, Mass). Peptides were reconstituted in 0.1% formic acid quantified with a modified Micro Lowry assay (kit from Sigma-Aldrich), and nearly 2  $\mu$ g was loaded through Acclaim PepMap 100 trap columns (75  $\mu$ m inner diameter  $\times$  2 cm) using a FAMOS autosampler (Thermo Fisher Scientific). Peptides were separated with an EASY-Spray PepMap C18 column (25 cm  $\times$  75  $\mu$ m with 2- $\mu$ m particles and 100 Å pore size) (Thermo Fisher Scientific), applying a 2% to 50% gradient of B over 60 minutes after 15 minutes of isocratic elution at 2% B and a constant flow rate of 300 nL/minute. Eluent A was 0.1% formic acid (vol/vol) in LC-MS-grade water, and eluent B was 0.1% formic acid (vol/vol) in 80% acetonitrile. MS1 precursor spectra were acquired in the positive ionization mode, scanning the mass-to-charge ratio range of 300 to 1600 with a resolving power of 70,000 full width at half maximum, an automatic gain control target of  $1 \times 10^6$  ions, and maximum

ion injection time of 120 ms. The spectrometer operated in data-dependent acquisition mode, selecting up to the 10 most intense ions for MS/MS fragmentation and applying a 12-second dynamic exclusion. The fragmentation of monocharged ions was allowed, while selection of background ions was impeded with an exclusion list, which was prepared based on the peak list obtained from a blank HPLC-MS/MS analysis. Spectra were elaborated using the software Xcalibur version 3.1 (Thermo Fisher Scientific). Digests of BSA-AGE were analyzed in triplicate in comparison with digests from unglycated BSA. Peptides were identified from LC-MS/MS runs using the Andromeda search engine of MaxQuant version 1.6.2.10 (<https://www.maxquant.org/>) against the BSA sequence (UniProt Knowledgebase accession P02769). Searching parameters were the following: no modification of cysteines, Met oxidation and pyroglutamic acid at the N terminus of Gln as variable modifications. Ne-(carboxymethyl) lysine (CML) (isobaric with glyoxal/arginine-derived hydroimidazolones, mass shift 58.0055 d) or Ne-(1-carboxyethyl) lysine (CEL) (isobaric with methylglyoxal/arginine-derived hydroimidazolones, mass shift 72.0011 d) were considered as possible variable modifications at uncleaved K or R. No enzyme cleavage specificity was set up. Mass tolerance default Andromeda values were used for the tolerance of precursor ion and MS/MS fragments. For the search of cross-linked peptides, the raw files were converted into Mascot Generic Format file and analyzed with the Batch Tag Web tool of the open source ProteinProspector search engine (<https://prospector.ucsf.edu>).

### Human enterocyte cell line

We used a well-validated model of human enterocytes, the Caco-2 cells (ATCC, Middlesex, United Kingdom; accession number HTB-37). These cells have the typical features of small intestine human enterocytes,<sup>41</sup> and they are commonly used for experiments exploring the effects of different substances on human intestine.<sup>40,42</sup> The cells were grown in Dulbecco modified Eagle medium with a high glucose concentration (4.5 g/L) and L-glutamine, supplemented with 10% FBS, 1% nonessential amino acids, 1% sodium pyruvate, and 1% penicillin/streptomycin (all Thermo Fisher Scientific). The cells were incubated at 37°C in a humidified atmosphere containing 5% carbon dioxide. The culture was changed every 2 days.

### Isolation of peripheral mononuclear blood cells

Peripheral blood samples (8 mL) were obtained from 4 children (White male, age range 48-60 months, with a positive family history for allergy in first-degree family members) consecutively observed at our center for minor surgical procedures. Blood samples were analyzed in an anonymized manner with the permission of the ethics committee of our institution. Informed written consent was obtained from parents or guardians of each subject. PBMCs were isolated by Ficoll density gradient centrifugation (Ficoll Histopaque-1077; Sigma-Aldrich). Briefly, cells were stratified on 3 mL of Ficoll and centrifuged 15 minutes at 1000g at room temperature. After centrifugation, the opaque interface containing mononuclear cells was carefully aspirated with a Pasteur pipette, and cells were washed with 10 mL of PBS and centrifuged 10 minutes at 500g at room temperature. After centrifugation, the upper layer was discarded, and PBMCs were collected.

### Cells stimulation protocol and RAGE inhibition

Caco-2 cells after 15 days postconfluence ( $1 \times 10^6$  cells/well) and PBMCs ( $2 \times 10^5$  cells/well) were stimulated at different doses (10-1000  $\mu\text{g/mL}$  of AGE-BSA or BSA) and times (24 hours and 48 hours). The results of these experiments suggested 200  $\mu\text{g/mL}$  of AGE-BSA for 48 hours as the most effective experimental condition for all variables tested. As demonstrated by a recent study,<sup>43</sup> 200  $\mu\text{g/mL}$  represents a plausible AGEs dose that would be encountered by human cells in real life. A similar concentration was adopted in previous studies performed by others.<sup>18,28,30,35</sup> The cells treated with only medium or with BSA, used as the nonglycated counterpart, were adopted as negative controls. Afterward, the supernatants were harvested and stored at  $-80^\circ\text{C}$  for further use.

In RAGE inhibition experiments, PBMCs ( $2 \times 10^5$  cells/well) were pretreated with 4  $\mu\text{g/mL}$  of RAGE neutralization antibody (#ab37647; AbCam) and with 4  $\mu\text{g/mL}$  of IgG Isotype Control (#ab206215; AbCam) and only medium as controls for 1 hour at 37°C and then were stimulated with 200  $\mu\text{g/mL}$  of AGE-BSA for 48 hours. After treatment, the supernatants were collected for cytokine analysis, and the cells were washed and harvested for flow cytometry analysis.

### Cell apoptosis rate evaluation by flow cytometry

Cell apoptosis rate was measured on stimulated Caco-2 cells and PBMCs, using Invitrogen Annexin V Apoptosis Detection Kit FITC (Thermo Fisher Scientific) according to the manufacturer's protocol. In brief, after washing with PBS, the collected cells were incubated with  $1 \times$  annexin V binding buffer. Then,  $3 \times 10^5$  cells were stained with annexin V fluorescein isothiocyanate (FITC) for 15 minutes at room temperature in the dark, and before reading, propidium iodide 5  $\mu\text{g/mL}$  was added to flow cytometer. Each sample was acquired using BD FACSCanto II flow cytometer and analyzed by BD FACSDiva software (BD Biosciences, Franklin Lakes, NJ). All experiments were carried out in duplicate.

### Transepithelial electrical resistance

To evaluate the monolayer integrity by transepithelial electrical resistance (TEER),  $2 \times 10^6$  Caco-2 cells per well were seeded on polycarbonate 6-well Transwell membranes (Corning Life Sciences, Kennebunk, Maine). After 15 days post-confluence, the TEER of the monolayer was measured every 24 hours for a total of 72 hours using an epithelial Millicell ERS-2 Volt ohmmeter (EMD Millipore, Billerica, Mass). Transepithelial resistance was measured at 24, 48, and 72 hours after AGE stimulation. The measured resistance value was multiplied by the area of the filter to obtain an absolute value of TEER, expressed as  $\Omega/\text{cm}^2$ , and the TEER values were measured as follows:  $\text{TEER} = (\text{measured resistance value} - \text{blank value}) \times \text{single cell layer surface area} (\text{cm}^2)$ .

### Measurement of intestinal permeability

To investigate the effect of AGEs on intestinal permeability, we used 4000 d FITC-labeled dextran (FD-4) as previously described.<sup>44</sup> Briefly, stimulated Caco-2 monolayers were washed twice with PBS, and after removing the medium, the cells were treated with FD-4 solution (1 mg/mL) on the apical

side and were incubated at 37°C for 2 hours. After the 2-hour treatment, samples (200  $\mu$ L) were taken under sink conditions at 0, 60, 120, and 180 minutes from the basolateral side. The amount of FD-4 was determined using a 96-well plate fluorescence reader (Universal Microplate Analyzer, Model AOPUS01 and AI53601; Packard BioScience, Meriden, Conn) with the excitation and emission wavelengths of 400 and 535 nm, respectively. Results were expressed as relative intensity.

### Transport and release assays

For transepithelial transport and release measurement to assess the gut barrier integrity, Caco-2 cells were pretreated with AGE and BSA (200  $\mu$ g/mL) for 48 hours. Then,  $\beta$ -lactoglobulin (BLG) (500  $\mu$ g/mL) and ovalbumin (OVA) (500  $\mu$ g/mL) were added to the apical side of the cells. After 24 hours, apical and basal media were collected for the BLG and OVA determination, using a commercially available specific ELISA kit (MyBioSource, Kampenhout, Belgium; detection limit of 0.05 ng/mL for BLG and 6 pg/mL for OVA).

### Quantitative real-time PCR

Total RNA was extracted from stimulated Caco-2 cells with TRIzol reagent and reverse transcribed in cDNA with a High-Capacity RNA-to-cDNA Kit (Thermo Fisher Scientific) according to the manufacturer's instructions. cDNA was stored at  $-80^{\circ}\text{C}$  until use. Quantitative real-time PCR analysis was performed using Taqman Gene Expression Master Mix (Thermo Fisher Scientific) to evaluate the effects of intestinal exposure to AGE-BSA or BSA on the gene expression of tight junction (TJ) proteins occludin (Hs00170162\_m1), and ZO-1 (Hs05378890\_cn), involved in the regulation of barrier integrity. The Taqman probes for these genes were inventoried and tested by Applied Biosystems at the Thermo Fisher Scientific manufacturing facility in Grand Island, NY (quality control). The amplification protocol was 40 cycles of 15 seconds of denaturation at  $95^{\circ}\text{C}$ , 60 seconds of annealing at  $60^{\circ}\text{C}$ , and 60 seconds of elongation at  $60^{\circ}\text{C}$  in an Applied Biosystems Light Cycler 7900HT (Thermo Fisher Scientific). Data were analyzed using the comparative threshold cycle method. We used the *GADPH* gene (Hs00483111\_cn) to normalize the level of mRNA expression.

### Assessment of IL-25, IL-33, and thymic stromal lymphopoietin

The epithelial cell-derived danger signal mediators, IL-25, IL-33, and thymic stromal lymphopoietin (TSLP), were assessed using commercially available ELISA kits specific for human IL-25 (Elabscience Biotech Co, Ltd, Wuhan, China; detection limit of 18.75 pg/mL), human IL-33 (BioVendor Research and Diagnostic Products, Brno, Czech Republic; detection limit of 0.2 pg/mL) and for human TSLP (Elabscience Biotech Co, Ltd; detection limit of 18.75 pg/mL) on the Caco-2 cell supernatants.

### Immunofluorescence and confocal microscopy

To investigate TJ proteins and RAGE receptor, Caco-2 cells were washed and fixed with ice-cold methanol and 4% paraformaldehyde, respectively, for 10 minutes at room temperature.

Then, the cells were washed twice with PBS and permeabilized with TERGITOL 15-S-9 (PanReac AppliChem) in PBS for 10 minutes. After washing, the cells were blocked for 1 h using 1% BSA in PBS/Tween 20 (PanReac AppliChem) and then incubated overnight at  $4^{\circ}\text{C}$  with specific primary antibody for occludin (1:100) (Abcam), ZO-1 (1:100) (Abcam), and RAGE (1:100) (AbCam; #37647). Coverslips were washed with PBS and incubated with fluorochrome conjugated secondary antibodies (1:200; Alexa Fluor 488; Thermo Fisher Scientific) for 1 hour at room temperature. Nuclei were stained with 4'-diamidino-2-phenylindole dihydrochloride (DAPI) (Thermo Fisher Scientific). Finally, cells were mounted in Mowiol. Glass slides were allowed to cure overnight in the dark. Cells were observed with 63 $\times$  objective on a Zeiss LSM980 confocal system equipped with an electronically switchable illumination and detection module and controlled by ZEN blue software (Carl Zeiss Microscopy GmbH, Jena, Germany). Fluorescence images presented are representative of cells imaged in at least 3 independent experiments.

### Reactive oxygen species production

Reactive oxygen species (ROS) production was measured using 7'-dichlorofluorescein diacetate (DCFH-DA) spectrofluorometric assay. After stimulation, cells were exposed to DCFH-DA 20  $\mu$ L (D6665; Sigma-Aldrich) for 30 minutes at  $37^{\circ}\text{C}$  in the dark, with 10 mM of  $\text{H}_2\text{O}_2$  (Sigma-Aldrich) used as a positive control. Intracellular ROS production was measured using a spectral fluorescence monitor (SFM 25; Kontron Instruments, Tokyo, Japan).

### Western Blot analysis

Total proteins were extracted from Caco-2 cells using RIPA Buffer (Thermo Fisher Scientific) following the manufacturer's instructions. The concentrations were determined by using a protein assay kit adopting BSA standards, according to the manufacturer's instructions (Bio-Rad Laboratories, Hercules, Calif). A total of 30  $\mu$ g protein was separated by SDS-PAGE, and blots were prepared on a nitrocellulose membrane (Immobilon-P PVDF Membrane; Merck, Darmstadt, Germany). The membranes were then incubated with anti-p-ERK 1/2 (#65142; Abcam), anti-nuclear factor- $\kappa$ B (NF $\kappa$ B) p65 (1:1000; sc-372, Santa Cruz Biotechnology, Dallas, Tex), anti-p(Ser 311)/p65-NF- $\kappa$ B (1:500; sc-101748; Santa Cruz Biotechnology), anti-LC3 (1:500; Novus Biologicals, Centennial, Colo; NB100-2220), anti-p62/SQSTM1 (1:1000; Sigma-Aldrich; P0067), anti-GAPDH (1:2000; Thermo Fisher Scientific; AM4300), anti- $\alpha$ -tubulin (1:5000; Sigma-Aldrich; T6074), and anti- $\beta$ -actin (ACTBD11B7; Santa Cruz Biotechnology) primary antibodies at different dilutions, overnight at  $4^{\circ}\text{C}$ . The peroxidase-linked (horseradish peroxidase) conjugated anti-rabbit IgG (1:2000; Abcam; ab205718) or anti-mouse IgG (1:5000; ImmunoReagents; Raleigh, NC; GtxMu-003-DHRPX) was used as a secondary antibody. Bound immunoglobulins were revealed by the enhanced chemiluminescence detection system, and the quantification was performed by ChemiDoc (Bio-Rad Laboratories). Densitometry analysis was obtained by the normalization to the band intensity of  $\alpha$ -tubulin,  $\beta$ -actin, GAPDH, and loading control, using Image Lab Software (Bio-Rad Laboratories).

## Duodenal organ culture and immunohistochemistry

Small intestinal biopsy specimens were collected by esophago-gastroduodenoscopy from 3 healthy subjects (all Caucasian males, mean age 17 years, range 15-18 years with a positive family history for allergy in first-degree family members) who had undergone endoscopy due to the presence of abdominal pain and/or diarrhea from at least 4 weeks and with normal endoscopic appearance of small intestine without histological inflammation. None of these subjects presented with organic conditions. Biopsy specimens were used to perform organ culture experiments as reported previously.<sup>45</sup> The biopsy culture was performed in RPMI-1640 medium (Sigma-Aldrich) without L-glutamine and supplemented with 10% fetal calf serum and antibiotic/antimycotic mixture (Thermo Fisher Scientific) for 24 hours at 37°C in medium alone or in presence of AGE (200 µg/mL) or BSA (200 µg/mL). The fragments were placed on a stainless steel mesh positioned over the central well of an organ culture dish with the villous surface of the specimens uppermost. After 24 hours of culture, the biopsy specimens were embedded in an optimal cutting temperature compound (Killik; Bio-Optica, Milan, Italy) and processed for immunohistochemistry as follows. Staining for activated mononuclear cells (CD25<sup>+</sup>) was performed using 4-µm frozen duodenal sections as previously reported.<sup>46</sup> The density of cells expressing CD25 in the lamina propria was evaluated within a total area of 1 mm<sup>2</sup>. The cutoff value was 4 cells/mm<sup>2</sup> lamina propria. Crypt epithelial cell proliferation was evaluated in cultured intestinal biopsy specimens by Ki-67 antigen detection as previously reported.<sup>46</sup> The number of Ki-67-positive cells in crypts divided by total crypt enterocytes resulted in the percentage of Ki-67-positive cells. All sections were evaluated with a light microscope Axioskop 2 Plus (Carl Zeiss Microscopy GmbH).

## Cell proliferation assay and RAGE analysis by flow cytometry

PBMCs were stained with carboxyfluorescein succinimidyl ester (CFSE) at final concentration of 2.5 µM (CellTrace CFSE Proliferation; Thermo Fisher Scientific) according to manufacturer's protocol. Briefly, the cells were incubated with CFSE for 15 minutes in darkness, stirring occasionally. Then, the reaction was stopped by adding PBS with 20% FBS, followed by centrifugation. This wash step was repeated 2 times. The stained cells were counted and seeded at  $2 \times 10^5$  cells/well in 200 µL of RPMI-1640 medium supplemented with 10% FBS, 1% L-glutamine, and 1% penicillin/streptomycin (all Lonza, Basel Switzerland) in a 96-well plate reader. The cells were treated for 48 hours with 200 µg/mL of AGE-BSA, or BSA or medium alone as negative controls. A portion of cells plated were treated with 1 µg/mL of PHA in combination with 200 µg/mL of AGE, or BSA or medium only as negative controls. After treatment, the supernatants were collected for cytokine analyses, and the cells were washed and harvested for flow cytometry analysis. The cells treated with PHA were also stained with anti-CD4 phycoerythrin monoclonal antibody (CYTOSENS, Naples, Italy).

To analyze surface expression of RAGE and to assess RAGE neutralization, Caco-2 cells and PBMCs were harvested, washed, and suspended in FCS buffer (ice-cold PBS, 0.1% fetal calf serum). Then, the cell suspension was plated in a 96-well U-bottom plate and labeled with recombinant Alexa Fluor 647

Anti-RAGE rabbit monoclonal antibody (Abcam; #ab237362) or the respective isotypes control antibody Recombinant Alexa Fluor 647 Rabbit IgG Isotype Control (Abcam; #199093), previously titrated. The cells were incubated at 4°C in the dark for 30 minutes, and after the incubation wash for 2 times with FACS buffer, before flow cytometer analysis. All phenotypes were analyzed with BD FACSCanto II system and elaborated using BD FACSDiva software.

## Assessment of T<sub>H</sub>1, T<sub>H</sub>2, and proinflammatory cytokines in PBMC culture supernatants

The concentrations of IL-4 and IL-10 were measured with a human IL-4/IL-10 enzyme immunoassay kit (Boster Biological Technology, Pleasanton, Calif). IL-5, IFN-γ, and IL-13 concentrations were measured using a human ELISA assay kit (Biovendor Research and Diagnostic Products). The minimum detection concentrations were 1.5 pg/mL for IL-4, 7.8 pg/mL for IL-5, 0.5 pg/mL for IL-10, 0.99 pg/mL for IFN-γ, and 0.7 pg/mL for IL-13. The concentrations of TNF-α and IL-6 were measured with a human ELISA kit (4.32 pg/mL for TNF-α and 1.6 pg/mL for IL-6) (Abcam). ELISAs were performed according to the manufacturer's recommendations.

## Mitochondrial function assessment by Seahorse XFp analyses

Mitochondrial metabolism in PBMCs was assessed by the Seahorse XFp analyzer (Agilent, Santa Clara, Calif), by using the Cell Mito Stress Test kit (#103010-100; Agilent). Before the Cell Mito Stress analyses, the cells were centrifuged at room temperature at 1200 rpm for 10 minutes, and the medium was replaced with a buffered base medium (Agilent Seahorse 103193) supplemented with 2 mM glutamine, 1 mM pyruvate, and 10 mM glucose at pH 7.4. In Seahorse miniplates, precoated with poly-D-lysine, 350,000 cells/well were seeded. The plate was centrifuged at 200g for 5 minutes at room temperature and equilibrated at 37°C in a carbon dioxide-free incubator for at least 1 hour. Basal oxygen consumption rate (OCR) was determined in the presence of glutamine (2 mM) and pyruvate (1 mM). The proton leak was determined after inhibition of mitochondrial ATP production by 1 µM oligomycin, as an inhibitor of F<sub>0</sub>-F<sub>1</sub> ATPases. Furthermore, measurement of ATP production in the basal state was obtained from the decrease in respiration by inhibition of the ATP synthase with oligomycin. Afterward, the mitochondrial electron transport chain was stimulated maximally by the addition of the uncoupler Trifluoromethoxy carbonyl cyanide phenylhydrazone, Carbonyl cyanide 4-(trifluoromethoxy)phenylhydrazone (1 µM). Coupling efficiency is the proportion of the oxygen consumed to drive ATP synthesis compared with that driving proton leakage and was calculated as the fraction of basal mitochondrial OCR used for ATP synthesis (ATP-linked OCR/basal OCR). Spare capacity is the capacity of the cell to respond to an energetic demand and was calculated as the difference between the maximal respiration and basal respiration. Mitochondrial respiration was expressed as the OCR per minute normalized to the number of cells. The data normalization of OCR can be performed in different ways to minimize inconsistency and variations from well to well.<sup>47</sup> The same cell number/well was plated before the OCR measurements; the cell count was obtained by using the Burkler chamber. Cell counting is a

nondestructive method to generate data for Seahorse normalization. In addition, at the end of analyses, we determined the protein content/well by Bradford assay and did not observe significant differences.

### Study participants

Consecutive pediatric patients (both sexes, age range 5-13 years) observed at our tertiary Program for Pediatric Allergy because of a recent diagnosis of FA were evaluated for the study. We excluded patients <5 or >13 years of age and patients presenting with tattoos or skin lesions/diseases; eosinophilic disorders of the gastrointestinal tract; allergic disorders other than FA; chronic systemic diseases; congenital cardiac defects; acute or chronic infectious diseases; autoimmune diseases; genetic and metabolic diseases; primary or secondary immunodeficiencies; inflammatory bowel diseases; celiac disease; food intolerances; obesity; neurologic and neuropsychiatric disorders; cystic fibrosis; malignancy; chronic pulmonary diseases; malformations of the gastrointestinal, respiratory, or urinary tract; history of gastrointestinal tract surgery; insufficient reliability or conditions that made compliance with the protocol unlikely; participation in other studies; and FA diagnosis obtained >4 weeks from evaluation. Thus, in all patients with FA, the diagnosis of FA was made in the last 4 weeks according to standard criteria<sup>48,49</sup> and were in stable clinical condition without symptoms attributable to FA when the AGE dietary intake and skin accumulation data were evaluated.

During the same study period, consecutive age-matched healthy children with negative history for any allergic condition who were visiting the center because of minor surgical procedures or vaccination were also evaluated for the study. Among the age-matched healthy children with a family risk for allergy (defined by the presence of  $\geq 1$  first-degree family members with allergy), 4 subjects were randomly selected for collecting PBMCs.

### Ethics

The study protocol, subject's information sheet, informed consent form, and clinical charts were reviewed and approved by the Ethics Committee of the University Federico II, Naples, Italy. The study was performed in accordance with the Helsinki Declaration (2004 Tokyo revision) and with the pertinent European and Italian regulations regarding privacy. The study was an observational study and was registered on [ClinicalTrials.gov](https://clinicaltrials.gov/ct2/show/results/NCT04273152) (<https://classic.clinicaltrials.gov/ct2/show/results/NCT04273152>), with the ClinicalTrials.gov Identifier NCT04273152.

### Data collection

At the baseline, after obtaining informed consent from the parents or guardians of each child, the anamnesis and the clinical status of the study children were carefully assessed by a multidisciplinary team composed of pediatricians, dietitians, and pediatric nurses to exclude children with concomitant comorbidities. Infectious diseases or other conditions were ruled out via a complete physical examination including vital signs; neurologic status; body growth status; nutritional status; hydration; skin evaluation; otoscopy; evaluation of oral cavity; respiratory, abdomen, and lymph node examination; and genital examination for pubertal staging. At enrollment, anamnestic,

demographic, anthropometric, and clinical data were obtained from the parents of each child and collected in a specific clinical chart. In addition, data on weekly frequency and duration of physical activity were collected in the clinical chart due to the evidence that lower levels of physical fitness could be associated with higher levels of skin AGEs.<sup>50</sup>

At study enrollment, after collection of written informed consent, the participants and their parents or guardians were asked to complete a 7-day (5 weekdays, 2 weekend days) food diary in the form of a printed chart to investigate dietary AGE intake.<sup>51</sup> Experienced pediatric dietitians explained to participants and to their parents or guardians about how to weigh foods and invited them to record in the food diary detailed information about food quantity, food preparation methods and times, ingredients of mixed dishes and recipes, and drinks consumed. To estimate the daily dietary AGE intake from the food diaries, a reference database of >200 food products commonly consumed in a Western diet built at the Maastricht University (Maastricht, The Netherlands) was used.<sup>9</sup> This database reports the content of the AGEs CML, CEL, and N $\delta$ -(5-hydro-5 methyl-4-imidazolone-2-yl)-ornithine (MG-H1), in milligrams per 100 g of food, quantified in the protein fractions of food products using highly specific ultra-performance LC-MS/MS. The daily dietary AGE intake was reported in the clinical chart.

### Assessment of skin autofluorescence

Selected AGEs have structural properties that cause them to emit fluorescent light across a specific range of wavelengths on excitation by UV light.<sup>52,53</sup> This unique characteristic has been used to develop a noninvasive device (AGE Reader; DiagnOptics Technologies BV, Groningen, The Netherlands) that quantifies accumulated AGEs within the human skin through the evaluation of skin autofluorescence (sAF) as previously described.<sup>54,55</sup> For the measurement, the participants were asked to place the dominant forearm on the device for 60 seconds. The AGE Reader illuminated a skin area of 4 cm<sup>2</sup> with UV-A light with a single peak excitation wavelength of 370 nm. Emission light (fluorescence in the wavelength of 420-600 nm) and reflected excitation light (with a wavelength of 300-420 nm) from the skin were measured using a spectrometer. Skin AGE levels were calculated as the ratio between the emission light and reflected excitation light, multiplied by 100 and expressed in arbitrary units. The intraday and interday coefficient was 2.6%. In all children, skin oils/ointments were not recently applied on the site of measurement before sAF measurement. Three measurements were performed on different sites of the skin on the volar side of the dominant forearm, as previously described.<sup>56</sup> The mean sAF value of the 3 measurements was reported.

### Data quality assurance

All data were recorded anonymously. At the study center, designated investigators were required to enter all collected data in the case report form. Two researchers performed separate checks of data completeness, clarity, consistency, and accuracy and instructed site personnel to make any required corrections or additions. Using a single data entry method, all data recorded in the case report form were entered in the study database by the same researcher. Then, the study dataset was reviewed and underwent data cleaning and verification according to standard

procedures. Finally, the database was locked once it was declared complete and accurate, and the statistical analysis was performed.

### Statistical analysis

The Kolmogorov-Smirnov test was used to determine whether variables were normally distributed. Descriptive statistics are reported as means  $\pm$  SDs for continuous variables or median and interquartile range, and discrete variables are reported as the number and proportion of participants with the characteristic of interest. To evaluate the differences among continuous variables, the independent sample *t* test or Mann-Whitney *U* test was performed. Differences among 3 groups were compared by one-way ANOVA test, followed by Tukey *post hoc* test. Differences were considered statistically significant at  $P < .05$ . Correlation analysis between skin AGE levels and age, sex, body mass index (BMI), and weekly duration of physical fitness was performed by Pearson correlation. All data were collected in a dedicated database and analyzed using IBM SPSS for Windows version 23.0 (IBM Corp, Armonk, New York).

## RESULTS

### Dietary AGEs could facilitate occurrence of FA through direct interaction with human cells

FA derives from a breakdown of the immune tolerance mechanisms.<sup>3</sup> In the first phase of our research, we focused on the direct effects elicited by AGEs on human cells assessing the most relevant nonimmune and immune variables involved in immune tolerance. For all experiments we used digested glycated BSA (AGE-BSA), a well-validated model of dietary AGEs<sup>19,24-28,30,32-35</sup> previously used in studies on a human enterocytes cell line (Caco-2 cells) and on PBMCs.<sup>18,22</sup> Before the experiments, AGE-BSA was digested in an infant gastrointestinal digestion model and monitored by SDS-PAGE (see Figs E1 and E2 in this article's Online Repository at [www.jacionline.org](http://www.jacionline.org)). The process is described in the Online Repository at [www.jacionline.org](http://www.jacionline.org).

### Apoptosis analysis by flow cytometry

To see whether AGEs could affect cell viability, we performed a double staining with annexin V and propidium iodide (PI). The exposure to AGEs increased the rate of necrotic (positive only for PI) and late apoptotic (positive for both PI and annexin V) cells (Fig E3 in the Online Repository at [www.jacionline.org](http://www.jacionline.org)).

### Alteration of gut barrier

The integrity of the gut barrier has a pivotal role in the maintenance of immune tolerance.<sup>57</sup> Human enterocytes exposed to AGEs showed an alteration of gut barrier integrity, as demonstrated by a reduction of TEER and by an increased permeability to FITC-labeled dextran (Fig 1, A and B). Exposure to AGEs caused an alteration of TJ proteins, as demonstrated by occludin and ZO-1 redistribution (Fig 1, C and D), and a reduction of their expression (Fig 1, C and D) in human enterocytes. These effects have been previously associated with TJ proteins alteration and barrier dysfunction in the intestinal epithelium.<sup>58</sup> To see whether these alterations could be responsible for an abnormal exposure to food antigens, we assessed BLG and OVA concentrations in the basal media of human

enterocyte cultures before and after AGEs exposure. We observed that the exposure to AGEs was able to elicit increased BLG and OVA passage across the gut barrier (Fig 1, E).

### Activation of epithelial cell-derived danger signal mediators

The epithelial cell-derived danger signal mediators, IL-25, IL-33, and TSLP, are often characterized as alarmins that are released by the gut epithelium in response to external insults and are responsible for driving T<sub>H</sub>2 cell-mediated response and allergic inflammation.<sup>59,60</sup> The exposure to AGEs elicited a significant increase of IL-25 and IL-33 production in human enterocytes compared with nontreated or BSA-treated cells (Fig 2, A and B). In contrast, no TSLP modulation was observed in cells exposed to AGEs (Fig 2, C).

### Activation of AGE-RAGE and autophagy pathways

Oxidative stress is involved in FA pathogenesis.<sup>61-64</sup> AGE-RAGE signaling has been shown to increase oxidative stress through extracellular signal-regulated kinase (ERK) 1/2 and NF- $\kappa$ B activation.<sup>65</sup> To analyze the intracellular mechanisms involved in the observed effects of AGEs in human enterocytes, we investigated RAGE expression, ROS production, and ERK1/2 and NF- $\kappa$ B activation. We found that stimulation with AGEs elicited a significant increase of RAGE and ROS production (Fig 3, A and B). Activation of RAGE was also confirmed by flow cytometry analyses (Fig E4 in the Online Repository at [www.jacionline.org](http://www.jacionline.org)). In addition, we observed that exposure to AGEs led to activation of signal transduction ERK1/2 and NF- $\kappa$ B in human enterocytes (Fig 3, C and D; Figs E5 and E6 in the Online Repository at [www.jacionline.org](http://www.jacionline.org)). As the existence of a crosstalk between the autophagic pathway and oxidative stress has been documented and that enhanced ROS production induces autophagy,<sup>66,67</sup> we also investigated the level of specific autophagic markers. We found that treatment with AGEs induced reduction of both the LC3-I/LC3-II ratio and p62/SQSTM1 levels in human enterocytes, suggesting an activation of the autophagic pathway (Fig 3, E; Fig E7 in the Online Repository at [www.jacionline.org](http://www.jacionline.org)).

### Effects of AGEs on inflammatory response in human small intestine organ culture

The proinflammatory action elicited by AGEs was also evaluated in experiments performed on small intestinal biopsy fragments collected by endoscopy from healthy children. Immunohistochemical analysis of AGE-treated small intestine cultures showed signs of activated mucosal inflammation (Fig 4, A). The density of lamina propria CD25<sup>+</sup> mononuclear cells resulted in significantly higher fragments stimulated with AGEs compared with fragments exposed to medium alone or to BSA (Fig 4, A and B). Early mucosa alteration in cultures stimulated with AGEs was also observed, as demonstrated by the higher rate of proliferating crypt enterocytes (Ki-67<sup>+</sup> cells) compared with both fragments exposed to medium alone or to BSA (Fig 4, C and D). The release of 2 proinflammatory cytokines, IL-6 and TNF- $\alpha$ , in the medium of small intestinal fragment cultures was also investigated. The exposure to AGEs induced a significant increase in production of these 2 inflammatory cytokines (Fig 4, E and F).

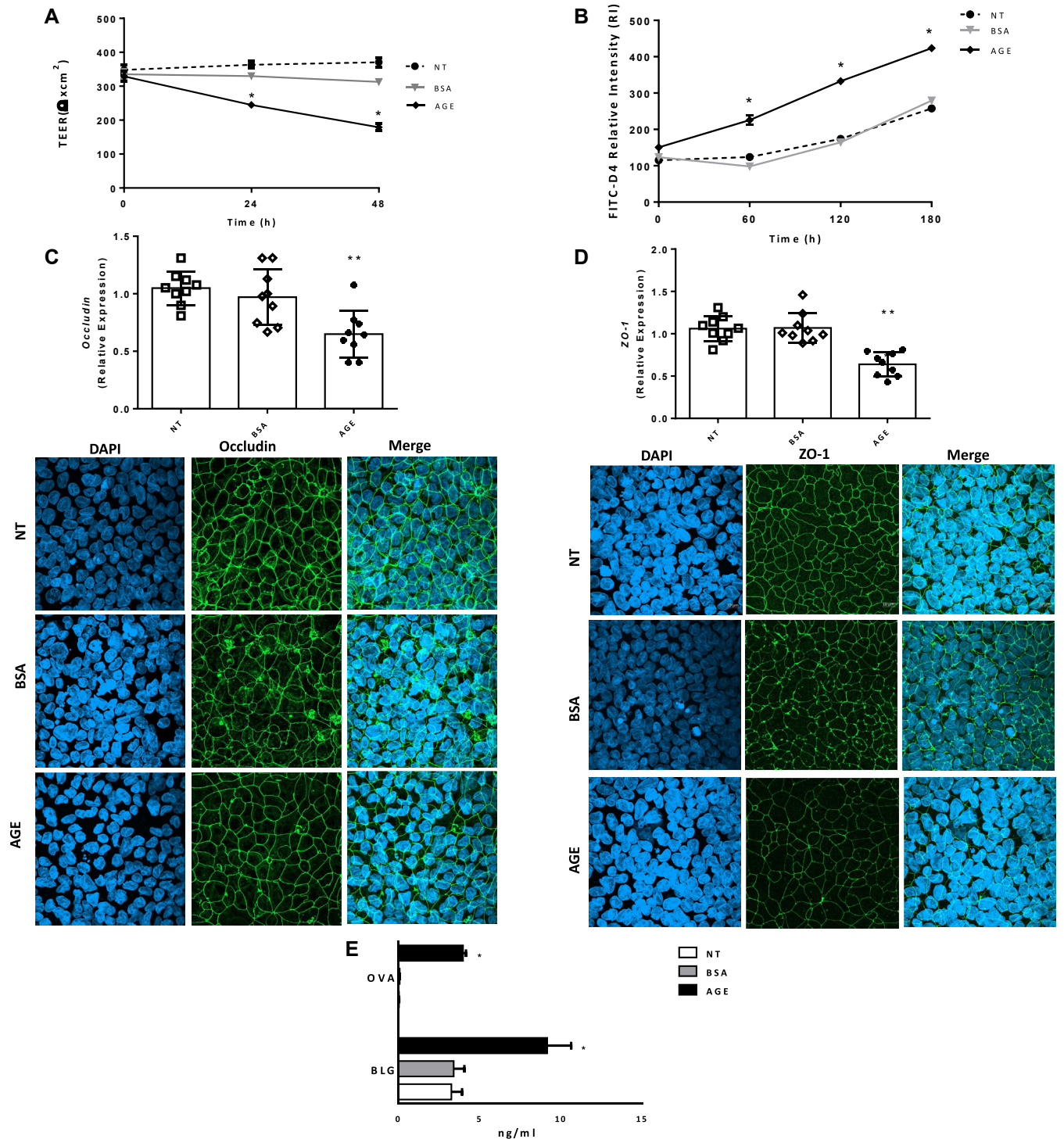


**FIG 1.** Effects of AGEs on gut permeability in human enterocytes. **(A)** Caco-2 cells were stimulated with AGEs or BSA at 200  $\mu\text{g}/\text{mL}$  for 48 hours. TEER values were measured as follows:  $\text{TEER} = (\text{measured resistance value} - \text{blank value}) \times \text{single cell layer surface area (cm}^2\text{)}$ . AGE stimulation affects intestinal permeability, as demonstrated by TEER measurement at up to 48 hours of incubation, compared with BSA-treated and nontreated cells. **(B)** Caco-2 cells were stimulated with AGEs or BSA at 200  $\mu\text{g}/\text{mL}$  for 48 hours. Then, the cells were treated with FD-4 solution (1 mg/mL) on the apical side and were incubated at 37°C for 2 hours. The amount of FD-4 was determined using a 96-well plate fluorescence reader and expressed as relative intensity. AGE stimulation affects intestinal epithelial permeability, as demonstrated by an increased permeability to FITC-dextran compared with BSA-treated and nontreated cells. **(C and D)** Caco-2 cells were stimulated with AGEs or BSA at 200  $\mu\text{g}/\text{mL}$  for 48 hours. Cells were processed for mRNA analysis by real-time PCR and fixed for immunofluorescence. Occludin (*C*, upper panel) and ZO-1 (*D*, upper panel) expression levels were significantly reduced in Caco-2 cells exposed to AGEs. Real-time PCR analysis



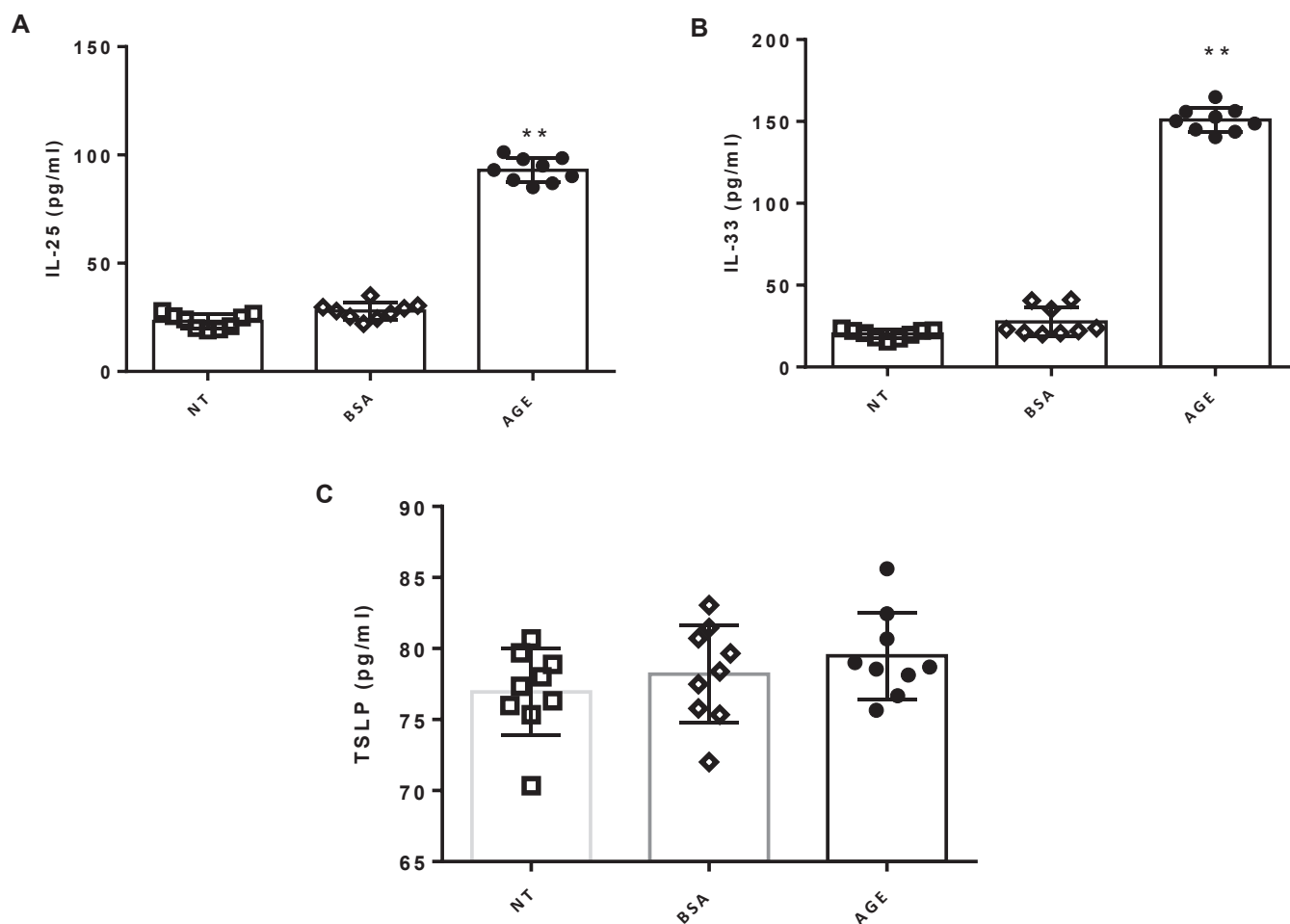


**FIG 2.** Effects of AGEs on activation of epithelial cell-derived danger signal mediators in human enterocytes. Caco-2 cells were stimulated with AGEs or BSA at 200  $\mu\text{g}/\text{mL}$  for 48 hours. IL-25, IL-33, and TSLP production were assessed by specific human ELISA kit. **(A and B)** Exposure to AGEs elicited a significant increase of IL-25 and IL-33 production compared with BSA treated and nontreated cells. **(C)** No modulation was observed in TSLP production in cells stimulated with AGEs. Data are expressed as means  $\pm$  SDs of 3 independent experiments, each performed in triplicate. Data were analyzed using one-way ANOVA. \*\* $P < .001$  vs BSA-treated and nontreated cells. NT, Nontreated cells.

### Effects of AGEs on cell apoptosis, proliferation, and cytokines response in human PBMCs

To further assess the ability of AGEs to facilitate the occurrence of FA, we tested cell viability and cytokine response in PBMCs collected from children at risk for atopy. We observed the same negative effects on viability of PBMCs previously observed in human enterocytes exposed to AGEs. As shown in Fig 5, A and B, the exposure to AGEs induced a significant increase of late

apoptotic cells (positive for both PI and annexin V) and a significant reduction of proliferation rate of PBMCs. Furthermore, to strengthen the evidence that AGEs affect cell proliferation, we conducted an additional proliferation test, treating PBMCs for 48 hours with 1  $\mu\text{g}/\text{mL}$  of PHA, a mitogen,<sup>68</sup> with 200  $\mu\text{g}/\text{mL}$  of AGE-BSA or BSA or medium alone as negative controls. As shown in Fig E6, treatment with AGEs reduces the proliferation rate, demonstrated by the reduction of CFSE dilution peaks, compared with medium and BSA alone. The result was confirmed

was performed using the comparative Ct method. Gene expression was normalized against the expression of the reference gene *GADPH*. Immunofluorescence analysis demonstrated that AGE exposure elicited a significant redistribution of TJ proteins occludin (C, lower panel) and ZO-1 (D, lower panel) in Caco-2 cells compared with BSA-treated and nontreated cells. Occludin (C, lower panel) and ZO-1 (D, lower panel) were visualized using Alexa Fluor 488 (green), and nuclei were stained with DAPI (blue). Cells were observed through a confocal microscope in the zy plane. Representative images of immunofluorescence are shown. Scale bar, 10  $\mu\text{m}$ . **(E)** Caco-2 cells were pretreated with AGEs and BSA (200  $\mu\text{g}/\text{mL}$ ) for 48 hours. Then, BLG (500  $\mu\text{g}/\text{mL}$ ) and OVA (500  $\mu\text{g}/\text{mL}$ ) were added to the apical side of the cells. After 24 hours, the basal media were collected for BLG and OVA determination. We observed that exposure to AGEs was able to elicit increased BLG and OVA transepithelial passage. Data are expressed as means  $\pm$  SDs of 3 independent experiments, each performed in triplicate. Data were analyzed using one-way ANOVA. \* $P < .05$ , \*\* $P < .001$  vs BSA-treated and nontreated cells. NT, Nontreated cells.

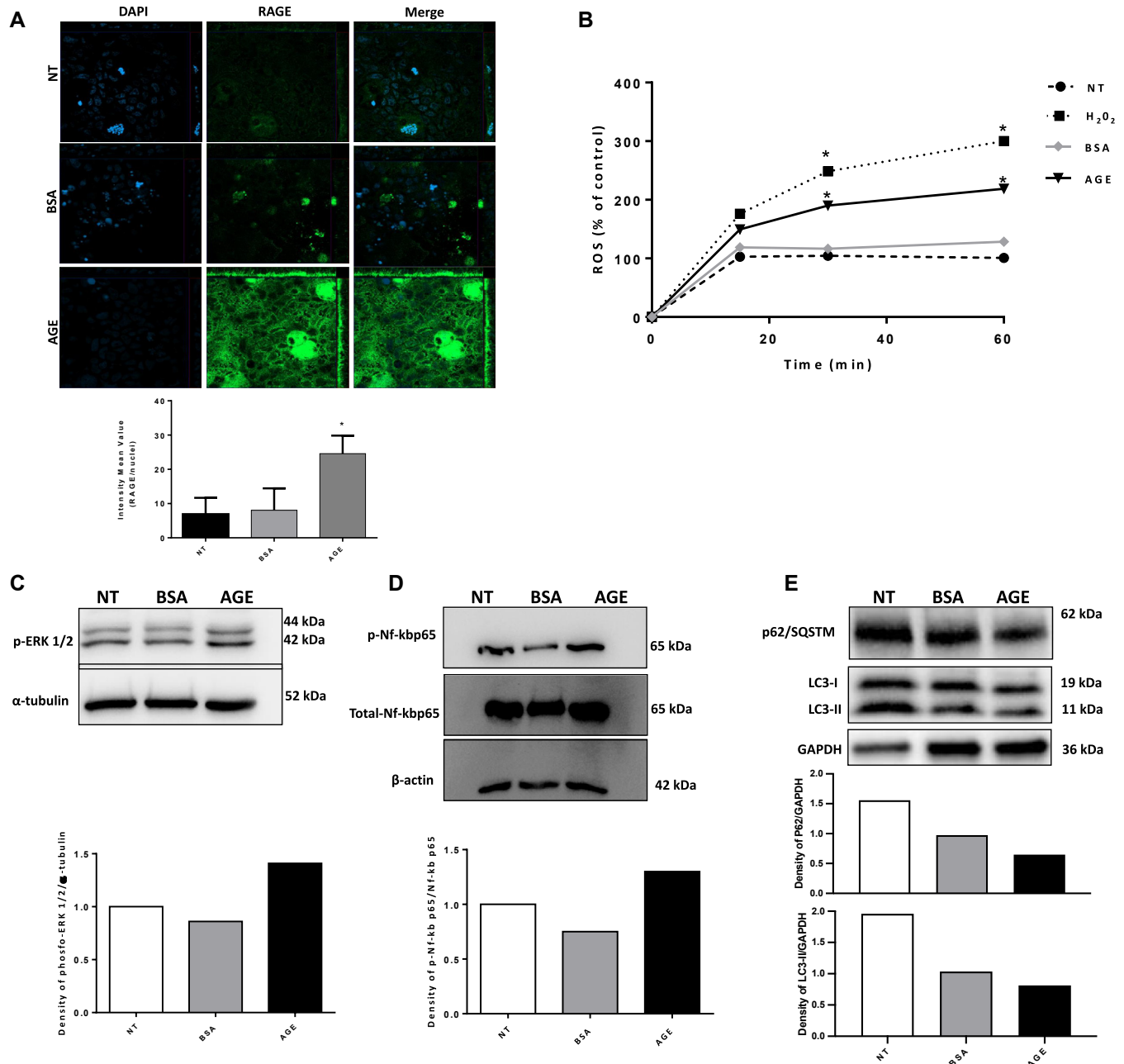


**FIG 3.** Effects of AGEs on activation of AGE-RAGE and autophagy pathways in human enterocytes. **(A)** Caco-2 cells were stimulated with AGEs or BSA at 200  $\mu$ g/mL for 48 hours. Cells were fixed and processed for immunofluorescence. RAGE was visualized using RAGE Alexa Fluor 488 (green), and nuclei were stained with DAPI (blue). AGE treatment increased RAGE expression compared with BSA-treated and nontreated cells. Representative images are shown. Scale bar, 10  $\mu$ m. **(B)** Caco-2 cells were stimulated with AGEs or BSA at 200  $\mu$ g/mL for 48 hours. ROS production was measured using DCFH-DA spectrofluorometry. AGE exposure elicited a significant increase in ROS production in a time-dependent manner. H<sub>2</sub>O<sub>2</sub> was a positive control. **(C–E)** Caco-2 cells were stimulated with AGEs or BSA at 200  $\mu$ g/mL for 48 hours. Western blot assay of phosphorylated ERK1/2 (pERK1/2) (C), NF- $\kappa$ B p65 (D), and LC3 and p62/SQSTM1 (E) was performed on protein extracts from Caco-2 cells. AGE exposure induced ERK1/2, NF- $\kappa$ B-p65 activation, LC3, and p62/SQSTM1 compared with BSA-treated and nontreated cells. The amounts of proteins  $\alpha$ -tubulin,  $\beta$ -actin, and GAPDH were measured by Western blot. The histogram below the Western blot shows optical density of the proteins, obtained with Image Lab Software. Relative quantification of proteins was normalized vs  $\alpha$ -tubulin for ERK,  $\beta$ -actin for NF- $\kappa$ B-p65, and GAPDH for LC3 and p62/SQSTM1 protein and was calculated using the ratio between phosphorylated and total proteins. The figures show representative images of 3 experiments qualitatively similar. Data are expressed as means  $\pm$  SDs of 3 independent experiments, each performed in triplicate. Data were analyzed using one-way ANOVA. \* $P$  < .05 vs BSA-treated and nontreated cells. NT, Nontreated cells.

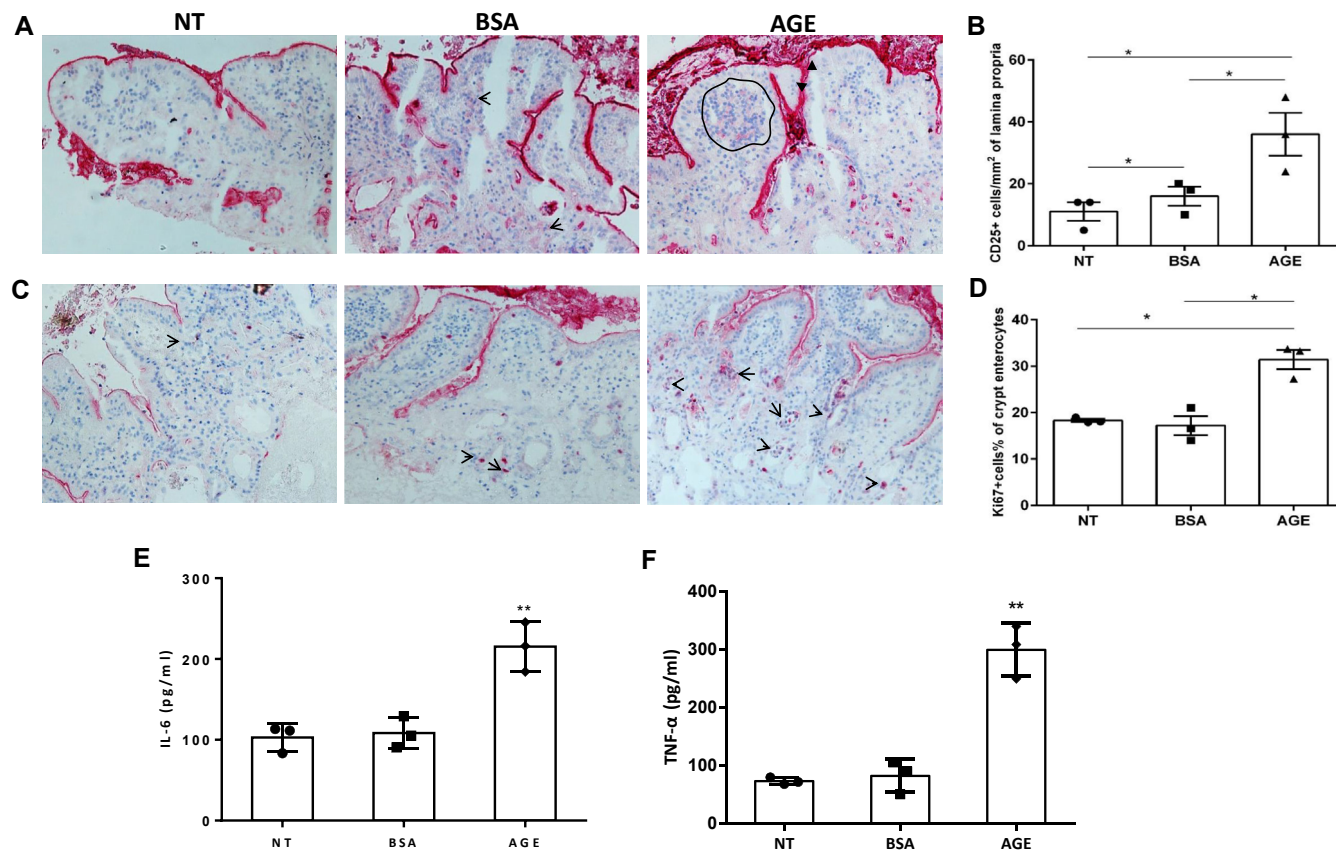


**FIG 4.** Effects of AGEs on inflammatory response in human small intestine organ culture. **(A)** Small intestinal biopsy fragments were exposed to AGEs or BSA at 200  $\mu\text{g}/\text{mL}$  for 24 hours. The fragments were processed for immunostaining of mononuclear CD25<sup>+</sup> cells in lamina propria of sections from cultured duodenal fragments. The activated cells are grouped under the epithelium in fragments treated with AGEs (cells surrounded by the *black line*). A few single CD25<sup>+</sup> cells are shown in fragments treated with BSA (*arrows*). Magnification  $\times 200$ . **(B)** Graph reporting density of CD25<sup>+</sup> cells/ $\text{mm}^2$  of lamina propria in small intestinal fragments cultured for 24 hours with AGEs or BSA-treated or nontreated cell fragments. **(C)** Immunostaining of Ki-67<sup>+</sup> cells in crypts in fragments treated with AGEs (*arrows*) or with BSA-treated or nontreated fragments. **(D)** Graph reporting the rate of proliferating crypt enterocytes expressed as percentage of Ki-67<sup>+</sup> crypt enterocytes. **(E and F)** Exposure to AGEs induced a significant increase of IL-6 (*E*) and TNF- $\alpha$  (*F*) production in the medium of duodenal fragments compared with BSA-treated or nontreated fragments. Data are expressed as means  $\pm$  SDs of 3 independent experiments and were analyzed using one-way ANOVA. \* $P < .05$ , \*\* $P < .001$  vs BSA-treated and nontreated cells. NT, Nontreated cells.

both by analyzing the total population of PBMCs (Fig E8, A, in the Online Repository at [www.jacionline.org](http://www.jacionline.org)) and by selecting CD4<sup>+</sup> T cells with an anti-CD4 phycoerythrin monoclonal antibody (Fig E8, B).

An increased production of T<sub>H</sub>2 (IL-4, IL-5, IL-13) and proinflammatory (IL-6, TNF- $\alpha$ , IFN- $\gamma$ ) cytokines was also observed in PBMCs exposed to AGEs (Fig 5, C-H). No modulation was detected for IL-10 production (Fig 5, J). These effects were mediated by RAGE activation (Fig 5, J), as demonstrated by the experiments of RAGE inhibition (Fig E9, A-D, in the Online Repository at [www.jacionline.org](http://www.jacionline.org)).

### Effects of AGEs on mitochondrial function in PBMCs

Emerging evidence suggests that mitochondrial dysfunction, and the consequent excessive generation of ROS, could be related to response of T<sub>H</sub>2 cytokines in FA.<sup>23</sup> We investigated the effects

of AGEs on mitochondrial function in PBMCs collected from children at risk for atopy. We found that the exposure to AGEs induced an alteration of mitochondrial metabolism in PBMCs (Fig 6, A). Specifically, we found that PBMCs exposed to AGEs showed a significant decrease of the basal and maximal respiration rate compared with nonexposed and BSA-exposed PBMCs (Fig 6, B and C). These results were consistent with the reduction of ATP production and spare respiratory capacity (ie, the cell competence to respond to increased energy demand or under stress) in AGE-treated cells (Fig 6, E and F). No modulation was observed for the mitochondrial proton leak and the coupling efficiency (Fig 6, D and G).

### Higher dietary AGE intake and skin AGE levels in children with FA

We also focused on the comparative evaluation of dietary AGE intake and skin AGE accumulation in children with FA and in

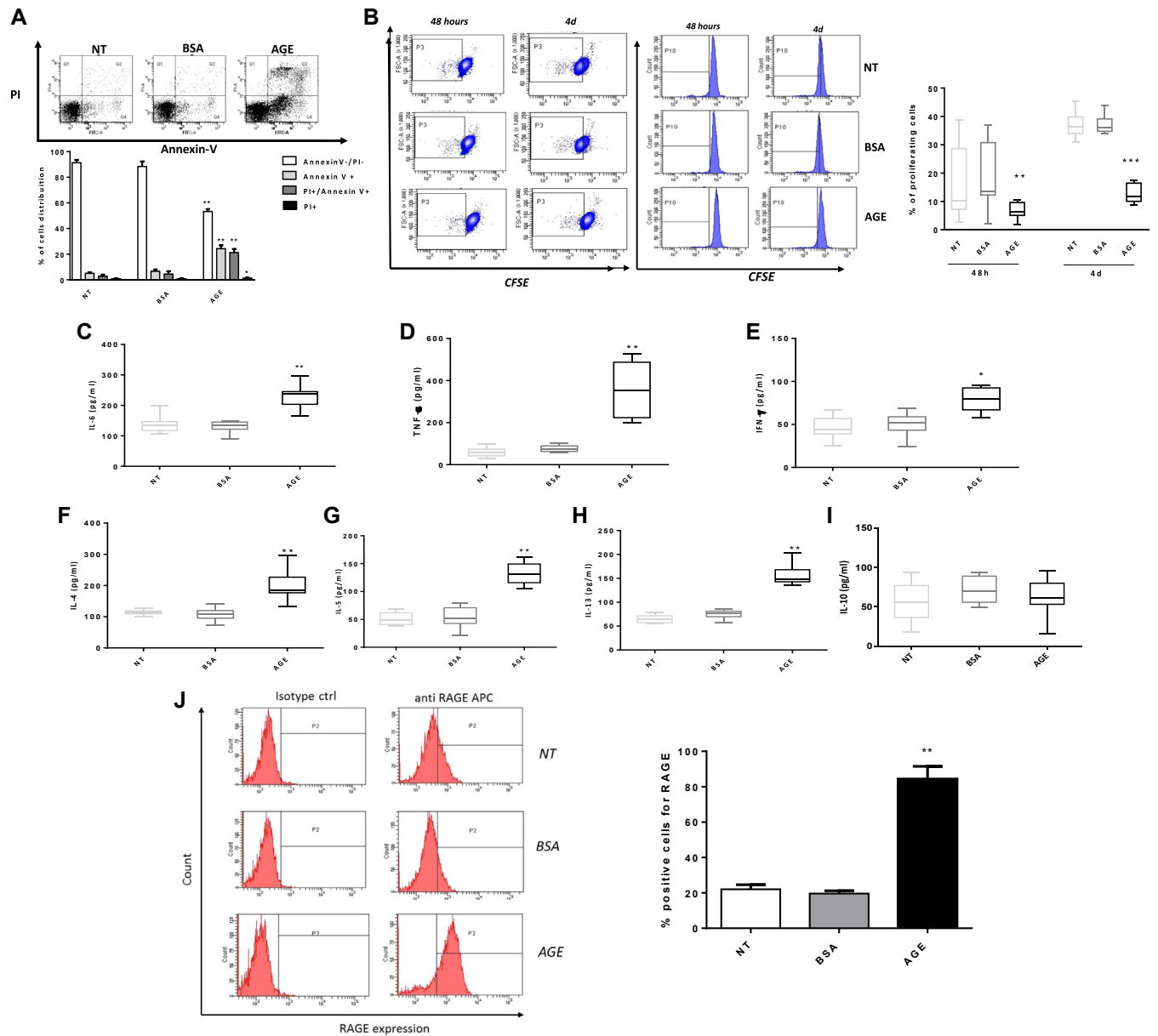


**FIG 5.** Effects of AGEs on cell apoptosis, proliferation,  $T_H2$ , tolerogenic and proinflammatory cytokines response, and RAGE activation in human PBMCs. PBMCs collected from 4 children at risk for atopic disorders were exposed to AGEs at 200  $\mu$ g/mL for 48 hours. Cells were harvested for flow cytometry analysis, and the supernatants were collected for analysis of cytokines. **(A)** Representative dot plots obtained by flow cytometric analysis after dual staining with annexin V-FITC and PI (upper panel). Exposure to AGEs induced a significant increase of late apoptotic cells (positive for both PI and Annexin V) (lower panel). Apoptosis and necrosis were quantified and expressed as percentage of cell distribution by flow cytometer after annexin V-FITC and PI labeling. **(B)** Representative dot plots and histograms of CFSE-labeled PBMCs. Exposure to AGEs elicited a significant reduction of proliferation rate of PBMCs (left panel). The proliferation rate was quantified and expressed as percentage of proliferating cells by flow cytometer after CFSE labeling (right panel). **(C–I)** Exposure of PBMCs to AGEs showed a significant increase of proinflammatory cytokines, IL-6 (C), TNF- $\alpha$  (D), and IFN- $\gamma$  (E), and of all  $T_H2$  cytokines production, IL-4 (F), IL-5 (G), and IL-13 (H). In contrast, no modulation was observed for IL-10 (I) production. **(J)** Representative dot plots obtained by flow cytometric analysis after labeling with recombinant Alexa Fluor 647 Anti-RAGE antibody and relative isotype control (left panel). Exposure of PBMCs to AGEs showed a significant increase of positive cells for RAGE (right panel). RAGE expression was quantified and expressed as percentage of positive cells by flow cytometer after labeling with recombinant Alexa Fluor 647 Anti-RAGE antibody. Data are expressed as means  $\pm$  SDs and were analyzed using one-way ANOVA. \* $P < .05$ , \*\* $P < .001$  vs BSA-treated and nontreated cells. ctrl, Control; NT, nontreated cells.

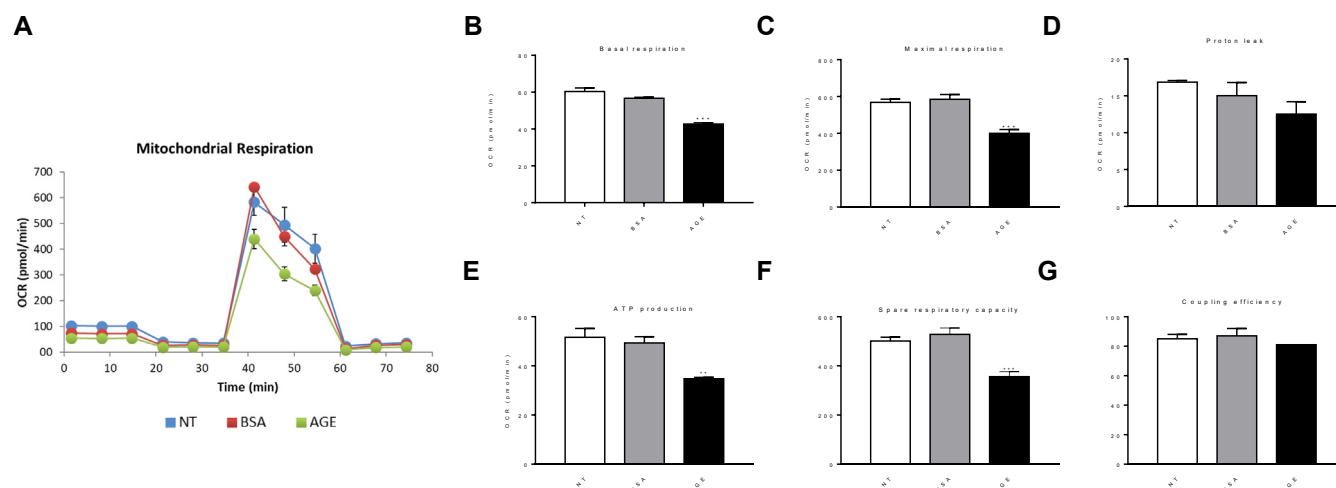


**FIG 6.** Assessment of mitochondrial respiration-linked parameters in human PBMCs exposed to AGEs. PBMCs collected from 4 children at risk for atopic disorders were exposed to AGEs or BSA at 200  $\mu$ g/mL for 48 hours. Cells were analyzed by the Seahorse XFp analyzer. **(A)** Representative graph of Cell Mito Stress assay performed by Seahorse XFp analyzer. Each point in the OCR time courses is the mean  $\pm$  SE of 2 technical replicates. **(B–G)** PBMCs exposed to AGEs showed a significant decrease of basal **(B)** and maximal **(C)** respiration rate and a significant reduction of ATP production **(E)** and the spare respiratory capacity **(F)**. No modulation was observed for the mitochondrial proton leak **(D)** and the coupling efficiency **(G)**. Data are expressed as means  $\pm$  SEs and were analyzed with one-way ANOVA. \*\* $P < .01$ , \*\*\* $P < .001$  vs BSA-treated and nontreated cells. NT, Nontreated cells.

age-matched HCs. From January 2018 to March 2020, 200 consecutive eligible subjects were evaluated for the study. After 60 subjects were excluded due to exclusion criteria, 140 subjects were invited to participate in the study, of whom 32 declined to participate. Thus, 108 children subdivided into 2 groups, 42 patients with FA and 66 HCs, were enrolled. All children were from families of middle socioeconomic status and lived in urban areas. The weekly duration of physical activity was similar in the groups. The main features of the study population are reported in Table I.

Considering that preclinical studies have shown that some dietary AGEs elicit proinflammatory and allergic effects,<sup>12</sup> the daily intake of the 3 most common glycation products in Western diet foods, CML, CEL, and MG-H1, was comparatively evaluated in the 2 study groups, using a database reporting the content of these dietary AGEs in several foods commonly consumed in Western countries.<sup>9</sup> We found that the daily dietary intake of CML, CEL, and MG-H1 was significantly higher in patients with FA compared with HCs (Fig 7, A). Concomitantly, children with FA demonstrated significantly higher skin AGE accumulation compared with HCs (Fig 7, B). No significant correlations with skin AGE levels were observed for age ( $r = 0.149$ ;  $P = .125$ ), sex ( $r = 0.099$ ;  $P = .306$ ), BMI ( $r = -0.095$ ;  $P = .329$ ), or weekly duration of physical activity ( $r = 0.164$ ;  $P = .171$ ).

## DISCUSSION

The prevalence of pediatric FA has increased in recent decades in the United States and in other westernized countries.<sup>1,69</sup> Potential drivers for this changing epidemiologic scenario, other than genetic predisposition, include several environmental factors, such as mode of delivery, exposure to drugs and pollution, and diet.<sup>3,70,71</sup> Dietary habits in the first years of life could be particularly relevant in influencing the occurrence of FA.<sup>72-75</sup>

Observational studies have suggested that a dietary pattern rich in AGE-containing UPFs is associated with increased prevalence of FA.<sup>76-78</sup>

FA depends on an alteration of mechanisms of immune tolerance.<sup>3</sup> Here, we explored the effects of AGEs on the main tolerogenic mechanisms involved in protecting children against FA.<sup>79</sup> Among nonimmune mechanisms, gut barrier integrity represents the first line of defense against external insults targeting epithelial cells, and it is of pivotal importance in preserving immune tolerance.<sup>57,80</sup> We demonstrated that AGEs had negative effects on gut epithelial barrier integrity as demonstrated by increased FITC-labeled dextran permeability, reduced TEER, and TJ protein expression. These effects were associated with an increased transepithelial passage of food antigens.

When epithelia are injured, danger signal molecules called alarmins are released.<sup>81</sup> AGEs mimic alarmins; through binding with RAGE, they induce the release of epithelial cytokine-derived danger signal mediators IL-33, IL-25, and TSLP.<sup>59</sup> Then, the production of IL-33 functions as an alarm warning of epithelial damage leading to  $T_H2$  cell activation.<sup>60</sup> We demonstrated that AGEs stimulate IL-33 production by human enterocytes. RAGE is the receptor of AGEs.<sup>82</sup> A pivotal mechanism by which interaction of AGEs and RAGE mediates oxidative cell stress and upregulates inflammatory pathways is via activation of ERK1/2 and NF- $\kappa$ B.<sup>83,84</sup> According to these findings, we found that RAGE activation is still present after AGE-BSA gastrointestinal digestion. This suggests that digested dietary glycosylated peptides can maintain the ability to interact with the receptors. As a consequence of RAGE activation, stimulation with AGEs increased ROS production and elicited ERK1/2 and NF- $\kappa$ B pathway activation in human enterocytes. Moreover, according to previous results,<sup>85</sup> we found that AGEs induced autophagy in human enterocytes. The negative impact of AGEs on human gut was also confirmed in experiments using small intestine organ

**TABLE I.** Baseline features of study participants

	FA patients (n = 42)	HCs (n = 66)
Sex, male, no. (%)	25 (59.5)	36 (54.5)
Age at enrollment (mo), mean $\pm$ SD	92.9 $\pm$ 23	103.5 $\pm$ 23.7
Cesarean delivery, no. (%)	24 (57.1)	41 (62.1)
Breastfeeding, no. (%)	33 (78.6)	48 (72.7)
Duration of breastfeeding (mo), mean $\pm$ SD	10.1 $\pm$ 10	7.7 $\pm$ 7.1
Exposure to passive smoking, no. (%)	6 (14.3)	25 (37.9)
Familial risk of allergy, no. (%)	34 (81)	17 (25.8)
First-degree relatives with allergy (count), median (IQR)*	1 (0)	1 (0)
Weight at enrollment (kg), mean $\pm$ SD	29.4 $\pm$ 11.9	34.6 $\pm$ 13.1
Height at enrollment (cm), mean $\pm$ SD	125.6 $\pm$ 14.4	133.7 $\pm$ 13
BMI at enrollment, kg/m <sup>2</sup> , mean $\pm$ SD	18 $\pm$ 3.6	18.7 $\pm$ 4.3
Physical activity, no. (%)	27 (64.3)	44 (66.7)
Physical activity at least 3 times per wk, mean $\pm$ SD	2.41 $\pm$ 0.8	2.8 $\pm$ 1.4
Total serum IgE (kU/L), mean $\pm$ SD	151.7 $\pm$ 87.1	0.1 $\pm$ 0.08
Gastrointestinal symptoms, no. (%)	31 (73.8)	—
Cutaneous symptoms, no. (%)	14 (33.3)	—
Respiratory symptoms, no. (%)	5 (11.9)	—

IQR, Interquartile range.

\*Calculated only for the subjects with familial risk of allergy.

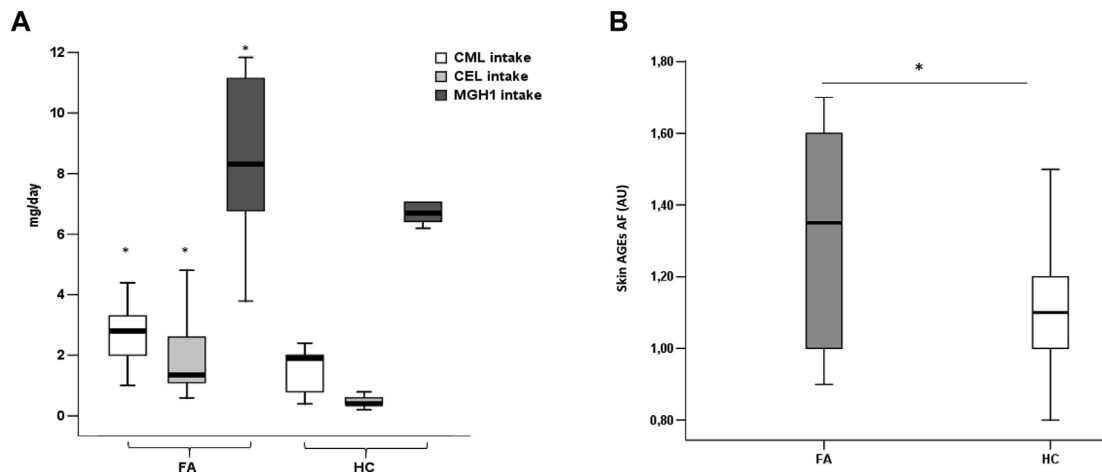


**FIG 7.** Evaluation of CML, CEL, and MG-H1 and skin AGEs levels in pediatric patients with FA and in HCs. **(A)** Median dietary intake of CML, CEL, and MG-H1 (mg/day) was significantly higher in patients with FA compared with HCs. **(B)** The median of sAF values in the study groups was reported. Significantly higher levels of skin AGEs were observed in patients with FA compared with HCs. Data are expressed as median and interquartile range. Data were analyzed using the Mann-Whitney *U* test. \**P* < .05 vs HCs. AU, Arbitrary units.

cultures, where we found early alteration of human intestinal mucosa stimulated with AGEs, characterized by increased number of CD25<sup>+</sup> mononuclear cells and increased rate of proliferation of crypt cells, biomarkers of intestinal mucosa inflammation and damage, respectively.<sup>86</sup>

Previous studies reported that RAGE is highly expressed on dendritic cells, macrophages, T lymphocytes, and B cells as well as mast cells and basophils.<sup>85,87</sup> In addition, it has been demonstrated that binding of AGEs to RAGE activates mast cells and generates histamine and oxidative stress products.<sup>88</sup>

The activation of NF- $\kappa$ B, mediated by AGEs and RAGE, leads to enhanced expression of vascular cell adhesion molecule 1 and intercellular adhesion molecule 1 on leukocytes and macrophages and production of proinflammatory cytokines such TNF- $\alpha$ , IL-1,

and IL-6.<sup>19,89</sup> In accordance with these findings, we observed higher production of inflammatory (IL-6, TNF- $\alpha$ , IFN- $\gamma$ ) and T<sub>H</sub>2 (IL-4, IL-5, IL-13) cytokines in PBMCs from children at risk for atopy and exposed to AGEs. These results are in line with previous data reporting that the stimulation of dendritic cells by AGEs resulted in T<sub>H</sub>2 cytokine response.<sup>17,37</sup> The ability of AGEs to elicit T<sub>H</sub>2 cytokine production in immune cells of at-risk children further supports the hypothesis that AGEs could facilitate the occurrence of FA. These effects were not involved in a modulation of IL-10 production.

The mitochondria, in addition to being the powerhouses of the cell, also represent the key regulators of immunity.<sup>17,90,91</sup> Preliminary data on a potential bidirectional cause-and-effect relationship between mitochondrial dysfunction and FA has been

previously reported in the animal model.<sup>61</sup> Here, we provided evidence that AGEs could alter the mitochondrial metabolism of human PBMCs as shown by the reduced basal respiration rate, ATP production, and spare respiratory capacity in AGE-treated cells. These effects could be responsible, at least in part, for the negative effects elicited by AGEs on viability of PBMCs, as previously suggested by other authors.<sup>92-94</sup>

Finally, we described a significantly higher dietary intake of AGEs and higher levels of skin AGE levels in pediatric patients with FA compared with age-matched HCs. This evidence further supports the potential role of AGEs in facilitating the occurrence of FA.

The major limitations of our study are the lack of measurements of plasmatic AGEs and soluble secretory RAGE in the study population, both of which have an important role in detoxification of AGEs in human body. Preliminary evidence suggested that the effects of AGEs could also involve epigenetic mechanisms through the activation of RAGE.<sup>94-98</sup> A study demonstrated that RAGE activation increased histone deacetylase 1 expression, inducing airway inflammation in a murine asthma model.<sup>99</sup> This could be a relevant aspect for clinical practice suggesting a long-lasting detrimental action of these compounds beyond childhood. Future studies are recommended to explore the epigenetic effects of the relationship of AGEs to the occurrence of FA and the effects of other components of UPFs, including emulsifiers, thickeners, and artificial sweeteners, that could have detrimental effects on immune tolerance mechanisms.<sup>100-103</sup>

In conclusion, this is the first study to our knowledge exploring how AGEs could facilitate the occurrence of FA. Using different experimental models, our data suggest that dietary AGEs, through a direct interaction with human cells, could have a negative impact on immune tolerance. Higher intake of dietary AGEs and subsequent skin accumulation of AGEs further support the hypothesis that increased exposure to dietary AGEs could facilitate pediatric FA. Dietary AGEs do not represent the only components of UPFs with detrimental effects on human health. Other UPF components, such as preservatives, sweeteners, color additives, flavors and spices, flavor enhancers, emulsifiers, leavening agents, anticaking agents, stabilizers, and thickeners, have been associated with adverse health outcomes in children.<sup>104-106</sup> Based on this evidence, lifestyle changes that include decreased consumption of ultraprocessed foods could be a promising strategy to prevent FA.

## DISCLOSURE STATEMENT

This study was supported by the Department of Translational Medical Science of the University of Naples Federico II, Naples, Italy, which received funding from the National Recovery and Resilience Plan, European Union–NextGenerationEU (On Foods–Research and Innovation Network on Food and Nutrition Sustainability, Safety and Security—Working on Foods; code PE0000003) and from the Italian Ministry of Health–Health Operational Plan Trajectory 5–Line of action “Creation of an action program for the fight against malnutrition in all its forms and for the dissemination of the principles of the diet Mediterranean” (Mediterranean Diet for Human Health Lab [MeDiHealthLab] No. T5-AN-07).

Disclosure of potential conflict of interest: The authors declare that they have no relevant conflicts of interest.

We thank the children and families for their participation in this study. We thank all physicians, nurses, technicians, and staff members for their enormous support during the study.

This article is dedicated to our invaluable colleague and friend, Professor Alberto Ritieni, an excellent scientist with a brilliant mind, who recently passed away.

**Clinical implications: Our findings suggest that lifestyle changes that include decreased consumption of ultraprocessed foods should be actively promoted to prevent FA.**

## REFERENCES

- Spolidoro GCI, Amara YT, Ali MM, Nyassi S, Lisik D, Ioannidou A, et al. Frequency of food allergy in Europe: an updated systematic review and meta-analysis. *Allergy* 2023;78:351-68.
- Loh W, Tang MLK. The epidemiology of food allergy in the global context. *Int J Environ Res Public Health* 2018;15:2043.
- Brough HA, Lanser BJ, Sindher SB, Teng JMC, Leung DYM, Venter C, et al. Early intervention and prevention of allergic diseases. *Allergy* 2022;77:416-41.
- Berni Canani R, Paparo L, Nocerino R, Di Scala C, Della Gatta G, Maddalena Y, et al. Gut microbiome as target for innovative strategies against food allergy. *Front Immunol* 2019;10:191.
- Lawrence MA, Baker PI. Ultra-processed food and adverse health outcomes. *BMJ* 2019;365:12289.
- Wang L, Martínez Steele E, Du M, Pomeranz JL, O'Connor LE, Herrick KA, et al. Trends in consumption of ultraprocessed foods among US Youths Aged 2-19 Years, 1999-2018. *JAMA* 2021;326:519-30.
- Zhang Q, Wang Y, Fu L. Dietary advanced glycation end-products: perspectives linking food processing with health implications. *Compr Rev Food Sci Food Saf* 2020;19:2559-87.
- Nursten HE. The Maillard Reaction: Chemistry, Biochemistry, and Implications. London: Royal Society of Chemistry; 2005.
- Scheijen JLM, Clevers E, Engelen L, Dagnelie PC, Brouns F, Stehouwer CDA, et al. Analysis of advanced glycation endproducts in selected food items by ultra-performance liquid chromatography tandem mass spectrometry: presentation of a dietary AGE database. *Food Chem* 2016;190:1145-50.
- Uribarri J, Cai W, Sandu O, Peppia M, Goldberg T, Vlassara H. Diet-derived advanced glycation end products are major contributors to the body's AGE pool and induce inflammation in healthy subjects. *Ann N Y Acad Sci* 2005; 1043:461-6.
- Clynes R, Moser B, Yan SF, Ramasamy R, Herold K, Schmidt AM. Receptor for AGE (RAGE): weaving tangled webs within the inflammatory response. *Curr Mol Med* 2007;7:743-51.
- Uribarri J, Cai W, Peppia M, Goodman S, Ferrucci L, Striker G, et al. Circulating glycotoxins and dietary advanced glycation endproducts: two links to inflammatory response, oxidative stress, and aging. *J Gerontol A Biol Sci Med Sci* 2007; 62:427-33.
- Sessa L, Gatti E, Zeni F, Antonelli A, Catucci A, Koch M, et al. The receptor for advanced glycation end-products (RAGE) is only present in mammals, and belongs to a family of cell adhesion molecules (CAMs). *PLoS One* 2014;9:e86903.
- Valencia JV, Mone M, Zhang J, Weetall M, Buxton FP, Hughes TE. Divergent pathways of gene expression are activated by the RAGE ligands S100b and AGE-BSA. *Diabetes* 2004;53:743-51.
- Smith PK, Masilamani M, Li XM, Sampson HA. The false alarm hypothesis: food allergy is associated with high dietary advanced glycation end-products and proglycating dietary sugars that mimic alarmins. *J Allergy Clin Immunol* 2017;139:429-37.
- Carucci L, Coppola S, Luzzetti A, Voto L, Giglio V, Paparo L, et al. Immunonutrition for pediatric patients with cow's milk allergy: how early interventions could impact long-term outcomes. *Front Allergy* 2021;2:676200.
- Briceno Noriega D, Zenker HE, Croes CA, Ewaz A, Ruinmans-Koerts J, Savelkoul HFJ, et al. Receptor mediated effects of advanced glycation end products (AGEs) on innate and adaptive immunity: relevance for food allergy. *Nutrients* 2022;14:371.
- Frasnelli SCT, de Medeiros MC, Bastos Ade S, Costa DL, Orrico SR, Rossa Junior C. Modulation of immune response by RAGE and TLR4 signalling in PBMCs of diabetic and non-diabetic patients. *Scand J Immunol* 2014;81:66-71.
- Shen CY, Wu CH, Lu CH, Kuo YM, Li KJ, Hsieh SC, et al. Advanced glycation end products of bovine serum albumin suppressed Th1/Th2 cytokine but enhanced monocyte IL-6 gene expression via MAPK-ERK and MyD88 transduced NF-κB p50 signaling pathways. *Molecules* 2019;24:2461.

20. Saha P, Kou JH. Effect of bovine serum albumin on drug permeability estimation across Caco-2 monolayers. *Eur J Pharm Biopharm* 2002;54:319-24.
21. Schmitt A, Nöller J, Schmitt J. The binding of advanced glycation end products to cell surfaces can be measured using bead-reconstituted cellular membrane proteins. *Biochim Biophys Acta* 2007;1768:1389-99.
22. Schmitt A, Bigl K, Meiners I, Schmitt J. Induction of reactive oxygen species and cell survival in the presence of advanced glycation end products and similar structures. *Biochim Biophys Acta* 2006;1763:927-36.
23. Suárez G, Rajaram R, Oronsky AL, Gawinowicz MA. Nonenzymatic glycation of bovine serum albumin by fructose (fructation). Comparison with the Maillard reaction initiated by glucose. *J Biol Chem* 1989;264:3674-9.
24. Rondeau P, Bourdon E. The glycation of albumin: Structural and functional impacts. *Biochimie* 2011;93:645-58.
25. Cai W, Torreggiani M, Zhu L, Chen X, He JC, Striker GE, et al. AGER1 regulates endothelial cell NADPH oxidase-dependent oxidant stress via PKC- $\delta$ : implications for vascular disease. *Am J Physiol Cell Physiol* 2010;298:C624-34.
26. Nagai R, Matsumoto K, Ling X, Suzuki H, Araki T, Horiuchi S. Glycolaldehyde, a reactive intermediate for advanced glycation end products, plays an important role in the generation of an active ligand for the macrophage scavenger receptor. *Diabetes* 2000;49:1714-23.
27. Chen CY, Abell AM, Moon YS, Kim KH. An advanced glycation end product (AGE)-receptor for AGEs (RAGE) axis restores adipogenic potential of senescent preadipocytes through modulation of p53 protein function. *J Biol Chem* 2012;287:44498-507.
28. Ju C, Sheng Z, Wang Q, Li Y, Wang X, Li S, et al. Advanced glycation end products of bovine serum albumin affect the cell growth of human umbilical vein endothelial cells via modulation of MEG3/miR-93/p21 pathway. *Acta Biochim Biophys Sin (Shanghai)* 2019;51:41-50.
29. Franke S, Sommer M, Rüster C, Bondeva T, Marticke J, Hofmann G, et al. Advanced glycation end products induce cell cycle arrest and proinflammatory changes in osteoarthritic fibroblast-like synovial cells. *Arthritis Res Ther* 2009;11:R136.
30. Lee JJ, Hsiao CC, Yang IH, Chou MH, Wu CL, Wei YC, et al. High-mobility group box 1 protein is implicated in advanced glycation end products-induced vascular endothelial growth factor A production in the rat retinal ganglion cell line RGC-5. *Mol Vis* 2012;18:838-50.
31. Yamagishi Si, Yonekura H, Yamamoto Y, Katsuno K, Sato F, Mita I, et al. Advanced glycation end products-driven angiogenesis in vitro. Induction of the growth and tube formation of human microvascular endothelial cells through autocrine vascular endothelial growth factor. *J Biol Chem* 1997;272:8723-30.
32. Subedi L, Lee JH, Gaire BP, Kim SY. Sulforaphane inhibits MGO-AGE-mediated neuroinflammation by suppressing NF- $\kappa$ B, MAPK, and AGE-RAGE signaling pathways in microglial cells. *Antioxidants (Basel)* 2020;9:792.
33. Münch G, Gasic-Milenkovic J, Dukic-Stefanovic S, Kuhla B, Heinrich K, Riederer P, et al. Microglial activation induces cell death, inhibits neurite outgrowth and causes neurite retraction of differentiated neuroblastoma cells. *Exp Brain Res* 2003;150:1-8.
34. Shen C, Ma Y, Zeng Z, Yin Q, Hong Y, Hou X, et al. RAGE-specific inhibitor FPS-ZMI attenuates AGEs-induced neuroinflammation and oxidative stress in rat primary microglia. *Neurochem Res* 2017;42:2902-11.
35. Shi L, Yu X, Yang H, Wu X. Advanced glycation end products induce human corneal epithelial cells apoptosis through generation of reactive oxygen species and activation of JNK and p38 MAPK pathways. *PLoS One* 2013;8:e66781.
36. Vissers YM, Blanc F, Skov PS, Johnson PE, Rigby NM, Przybylski-Nicaise L, et al. Effect of heating and glycation on the allergenicity of 2S albumins (Ara h 2/6) from peanut. *PLoS One* 2011;6:e23998.
37. Hilmenyuk T, Bellinghausen I, Heydenreich B, Ilchmann A, Toda M, Grabbe S, et al. Effects of glycation of the model food allergen ovalbumin on antigen uptake and presentation by human dendritic cells. *Immunology* 2010;129:437-45.
38. Taheri-Kafrani A, Gaudin JC, Rabesona H, Nioi C, Agarwal D, Drouet M, et al. Effects of heating and glycation of beta-lactoglobulin on its recognition by IgE of sera from cow milk allergy patients. *J Agric Food Chem* 2009;57:4974-82.
39. Paparo L, Picariello G, Bruno C, Pisapia L, Canale V, Sarracino A, et al. Tolerogenic effect elicited by protein fraction derived from different formulas for dietary treatment of cow's milk allergy in human cells. *Front Immunol* 2021;11:604075.
40. Holik AK, Lieder B, Kretschy N, Somoza MM, Ley JP, Hans J, et al. The advanced glycation end product N<sup>ε</sup>-carboxymethyllysine and its precursor glyoxal increase serotonin release from Caco-2 cells. *J Cell Biochem* 2018;119:2731-41.
41. Sambuy Y, De Angelis I, Ranaldi G, Scarino ML, Stammati A, Zucco F. The Caco-2 cell line as a model of the intestinal barrier: influence of cell and culture-related factors on Caco-2 cell functional characteristics. *Cell Biol Toxicol* 2005;21:1-26.
42. Bonvicini F, Pagnotta E, Punzo A, Calabria D, Simoni P, Mirasoli M, et al. Effect of *Lactobacillus acidophilus* fermented broths enriched with *Eruca sativa* seed extracts on intestinal barrier and inflammation in a co-culture system of an enterohemorrhagic *Escherichia coli* and human intestinal cells. *Nutrients* 2020;12:3064.
43. Zubchenko S, Kril I, Potemkina H, Havrylyuk A, Kuzan A, Gamian A, et al. Low level of advanced glycation end products in serum of patients with allergic rhinitis and chronic Epstein-Barr virus infection at different stages of virus persistence. *J Immunol Res* 2022;2022:4363927.
44. Kowapradit J, Opanasopit P, Ngawhirunpat T, Apirakaramwong A, Rojanarata T, Ruktanonchai U, et al. In vitro permeability enhancement in intestinal epithelial cells (Caco-2) monolayer of water soluble quaternary ammonium chitosan derivatives. *AAPS Pharm Sci Tech* 2010;11:497-508.
45. Paparo F, Petrone E, Tosco A, Maglio M, Borrelli M, Salvati VM, et al. Clinical, HLA, and small bowel immunohistochemical features of children with positive serum antiendomysium antibodies and architecturally normal small intestinal mucosa. *Am J Gastroenterol* 2005;100:2294-8.
46. Maglio M, Mazzarella G, Barone MV, Gianfrani C, Pogna N, Gazza L, et al. Immunogenicity of two oat varieties, in relation to their safety for celiac patients. *Scand J Gastroenterol* 2011;46:1194-205.
47. Divakaruni AS, Paradyse A, Ferrick DA, Murphy AN, Jastroch M. Analysis and interpretation of microplate-based oxygen consumption and pH data. *Methods Enzymol* 2014;547:309-54.
48. NIAID-Sponsored Expert Panel, Boyce JA, Assa'ad A, Burks AW, Jones SM, Sampson HA, et al. Guidelines for the diagnosis and management of food allergy in the United States: report of the NIAID-sponsored expert panel. *J Allergy Clin Immunol* 2010;126:S1-58.
49. Sicherer SH, Sampson HA. Food allergy: epidemiology, pathogenesis, diagnosis, and treatment. *J Allergy Clin Immunol* 2014;133:291-307.
50. Köchli S, Endes K, Trinkler M, Mondoux M, Zahner L, Hanssen H. Association of physical fitness with skin autofluorescence-derived advanced glycation end products in children. *Pediatr Res* 2020;87:1106-11.
51. Ortega RM, Pérez-Rodrigo C, López-Sobaler AM. Dietary assessment methods: dietary records. *Nutr Hosp* 2015;31(Suppl 3):38-45.
52. Monnier VM, Vishwanath V, Frank KE, Elmets CA, Dauchot P, Kohn RR. Relation between complications of type 1 diabetes mellitus and collagen-linked fluorescence. *N Engl J Med* 1986;314:403-8.
53. Obayashi H, Nakano K, Shigeta H, Yamaguchi M, Yoshimori K, Fukui M, et al. Formation of crossline as a fluorescent advanced glycation end product in vitro and in vivo. *Biochem Biophys Res Commun* 1996;226:37-41.
54. Mulder DJ, Water TV, Lutgers HL, Graaff R, Gans RO, Zijlstra F, et al. Skin autofluorescence, a novel marker for glycemic and oxidative stress-derived advanced glycation endproducts: an overview of current clinical studies, evidence, and limitations. *Diabetes Technol Ther* 2006;8:523-35.
55. Meerwaldt R, Links T, Graaff R, Thorpe SR, Baynes JW, Hartog J, et al. Simple noninvasive measurement of skin autofluorescence. *Ann N Y Acad Sci* 2005;1043:290-8.
56. Banser A, Naafs JC, Hoorweg-Nijman JJ, van de Garde EM, van der Vorst MM. Advanced glycation end products, measured in skin, vs. HbA1c in children with type 1 diabetes mellitus. *Pediatr Diabetes* 2016;17:426-32.
57. Velasquez-Manoff M. Gut microbiome: the peacekeepers. *Nature* 2015;518:S3-11.
58. Samak G, Narayanan D, Jaggar JH, Rao R. CaV1.3 channels and intracellular calcium mediate osmotic stress-induced N-terminal c-Jun kinase activation and disruption of tight junctions in Caco-2 cell monolayers. *J Biol Chem* 2011;286:30232-43.
59. Roan F, Obata-Ninomiya K, Ziegler SF. Epithelial cell-derived cytokines: more than just signaling the alarm. *J Clin Invest* 2019;129:1441-51.
60. Hong H, Liao S, Chen F, Yang Q, Wang DY. Role of IL-25, IL-33, and TSLP in triggering united airway diseases toward type 2 inflammation. *Allergy* 2020;75:2794-804.
61. Trinchese G, Paparo L, Aitoro R, Fierro C, Varchetta M, Nocerino R, et al. Hepatic mitochondrial dysfunction and immune response in a murine model of peanut allergy. *Nutrients* 2018;10:744.
62. Pattnaik B, Bodas M, Bhatraju NK, Ahmad T, Pant R, Guleria R, et al. IL-4 promotes asymmetric dimethylarginine accumulation, oxo-nitrative stress, and hypoxic response-induced mitochondrial loss in airway epithelial cells. *J Allergy Clin Immunol* 2016;138:130-41.
63. Kim SR, Kim DI, Kim SH, Lee H, Lee KS, Cho SH, et al. NLRP3 inflammasome activation by mitochondrial ROS in bronchial epithelial cells is required for allergic inflammation. *Cell Death Dis* 2014;5:e1498.
64. van Rijjt LS, Utsch L, Lutter R, van Ree R. Oxidative stress: promoter of allergic sensitization to protease allergens? *Int J Mol Sci* 2017;18:1112.



65. Waghela BN, Vaidya FU, Ranjan K, Chhipa AS, Tiwari BS, Pathak C. AGE-RAGE synergy influences programmed cell death signaling to promote cancer. *Mol Cell Biochem* 2021;476:585-98.
66. Filomeni G, De Zio D, Cecconi F. Oxidative stress and autophagy: the clash between damage and metabolic needs. *Cell Death Differ* 2015;22:377-88.
67. Tarallo A, Damiano C, Strollo S, Minopoli N, Indrieri A, Polishchuk E, et al. Correction of oxidative stress enhances enzyme replacement therapy in Pompe disease. *EMBO Mol Med* 2021;13:e14434.
68. Quah BJ, Wijesundara DK, Ranasinghe C, Parish CR. The use of fluorescent target arrays for assessment of T cell responses in vivo. *J Vis Exp* 2014;88:e51627.
69. Warren CM, Jiang J, Gupta RS. Epidemiology and burden of food allergy. *Curr Allergy Asthma Rep* 2020;20:6.
70. Lee KH, Song Y, Wu W, Yu K, Zhang G. The gut microbiota, environmental factors, and links to the development of food allergy. *Clin Mol Allergy* 2020;18:5.
71. Sikorska-Szaflik H, Sozańska B. Primary prevention of food allergy-environmental protection beyond diet. *Nutrients* 2021;13:2025.
72. Mazzocchi A, Venter C, Maslin K, Agostoni C. The role of nutritional aspects in food allergy: prevention and management. *Nutrients* 2017;9:850.
73. D'Auria E, Peroni DG, Sartorio MUA, Verduci E, Zuccotti GV, Venter C. The role of diet diversity and diet indices on allergy outcomes. *Front Pediatr* 2020;8:545.
74. Vassilopoulou E, Vardaka E, Efthymiou D, Pitsios C. Early life triggers for food allergy that in turn impacts dietary habits in childhood. *Allergol Immunopathol (Madr)* 2021;49:146-52.
75. Padilha LL, Vianna EO, Vale ATM, Nascimento JXPT, da Silva AAM, Ribeiro CCC. Pathways in the association between sugar sweetened beverages and child asthma traits in the 2nd year of life: findings from the BRISA cohort. *Pediatr Allergy Immunol* 2020;31:480-8.
76. Kim JH, Ellwood PE, Asher MI. Diet and asthma: looking back, moving forward. *Respir Res* 2009;10:49.
77. Manzel A, Muller DN, Hafler DA, Erdman SE, Linker RA, Kleinewietfeld M. Role of "Western diet" in inflammatory autoimmune diseases. *Curr Allergy Asthma Rep* 2014;14:404.
78. Brigham EP, Kolahdooz F, Hansel N, Breyse PN, Davis M, Sharma S, et al. Association between Western diet pattern and adult asthma: a focused review. *Ann Allergy Asthma Immunol* 2015;114:273-80.
79. Paparo L, Nocerino R, Ciaglia E, Di Scala C, De Caro C, Russo R, et al. Butyrate as a bioactive human milk protective component against food allergy. *Allergy* 2021;76:1398-415.
80. Thoo L, Noti M, Krebs P. Keep calm: the intestinal barrier at the interface of peace and war. *Cell Death Dis* 2019;10:849.
81. Bianchi ME. DAMPs, PAMPs and alarmins: all we need to know about danger. *J Leukoc Biol* 2007;81:1-5.
82. Schmidt AM, Vianna M, Gerlach M, Brett J, Ryan J, Kao J, et al. Isolation and characterization of two binding proteins for advanced glycosylation end products from bovine lung which are present on the endothelial cell surface. *J Biol Chem* 1992;267:14987-97.
83. Zill H, Günther R, Erbersdobler HF, Fölsch UR, Faist V. RAGE expression and AGE-induced MAP kinase activation in Caco-2 cells. *Biochem Biophys Res Commun* 2001;288:1108-11.
84. Marsche G, Semlitsch M, Hammer A, Frank S, Weigle B, Demling N, et al. Hypochlorite-modified albumin colocalizes with RAGE in the artery wall and promotes MCP-1 expression via the RAGE-Erk1/2 MAP-kinase pathway. *FASEB J* 2007;21:1145-52.
85. Verma N, Manna SK. Advanced glycation end products (AGE) potently induce autophagy through activation of RAF protein kinase and nuclear factor  $\kappa$ B (NF- $\kappa$ B). *J Biol Chem* 2016;291:1481-91.
86. Vitale S, Strisciunglio C, Pisapia L, Miele E, Barba P, Vitale A, et al. Cytokine production profile in intestinal mucosa of paediatric inflammatory bowel disease. *PLoS One* 2017;12:e0182313.
87. Liliensiek B, Weigand MA, Bierhaus A, Nicklas W, Kasper M, Hofer S, et al. Receptor for advanced glycation end products (RAGE) regulates sepsis but not the adaptive immune response. *J Clin Invest* 2004;113:1641-50.
88. Ramasamy R, Yan SF, Herold K, Clynes R, Schmidt AM. Receptor for advanced glycation end products: fundamental roles in the inflammatory response: winding the way to the pathogenesis of endothelial dysfunction and atherosclerosis. *Ann N Y Acad Sci* 2008;1126:7-13.
89. Sick E, Brehin S, André P, Coupin G, Landry Y, Takeda K, Gies JP. Advanced glycation end products (AGEs) activate mast cells. *Br J Pharmacol* 2010;161:442-55.
90. Reddy PH. Mitochondrial dysfunction and oxidative stress in asthma: implications for mitochondria-targeted antioxidant therapeutics. *Pharmaceuticals (Basel)* 2011;4:429-56.
91. Agrawal A, Mabalirajan U. Rejuvenating cellular respiration for optimizing respiratory function: targeting mitochondria. *Am J Physiol Lung Cell Mol Physiol* 2016;310:L103-13.
92. Mabalirajan U, Ghosh B. Mitochondrial dysfunction in metabolic syndrome and asthma. *J Allergy (Cairo)* 2013;2013:340476.
93. Aguilera-Aguirre L, Bacsí A, Saavedra-Molina A, Kurosky A, Sur S, Boldogh I. Mitochondrial dysfunction increases allergic airway inflammation. *J Immunol* 2009;183:5379-87.
94. Brookes PS, Yoon Y, Robotham JL, Anders MW, Sheu SS. Calcium, ATP, and ROS: a mitochondrial love-hate triangle. *Am J Physiol Cell Physiol* 2004;287:C817-33.
95. Perrone A, Giovino A, Benny J, Martinelli F. Advanced glycation end products (AGEs): biochemistry, signaling, analytical methods, and epigenetic effects. *Oxid Med Cell Longev* 2020;2020:3818196.
96. Kan S, Wu J, Sun C, Hao J, Wu Z. Correlation between RAGE gene promoter methylation and diabetic retinal inflammation. *Exp Ther Med* 2018;15:242-6.
97. Maslinska D, Laure-Kamionowska M, Maslinski S. Methyl-CpG binding protein 2, receptors of innate immunity and receptor for advanced glycation end-products in human viral meningoencephalitis. *Folia Neuropathol* 2014;52:428-35.
98. Zhang M, Li Y, Rao P, Huang K, Luo D, Cai X, et al. Blockade of receptors of advanced glycation end products ameliorates diabetic osteogenesis of adipose-derived stem cells through DNA methylation and Wnt signalling pathway. *Cell Prolif* 2018;51:e12471.
99. Peng X, Huang M, Zhao W, Lan Z, Wang X, Yuan Y, et al. RAGE mediates airway inflammation via the HDAC1 pathway in a toluene diisocyanate-induced murine asthma model. *BMC Pulm Med* 2022;22:61.
100. Cloonan SM, Choi AM. Mitochondria in lung disease. *J Clin Invest* 2016;126:809-20.
101. Mullen A. Ultra-processed food and chronic disease. *Nat Food* 2020;1:771.
102. Monteiro CA, Cannon G, Levy RB, Moubarac JC, Louzada ML, Rauber F, et al. Ultra-processed foods: what they are and how to identify them. *Public Health Nutr* 2019;22:936-41.
103. Calvo MS, Uribarri J. Food additive use in ultraprocessed foods: can processing use of industrial additives contribute to adverse health outcomes in children? *J Acad Nutr Diet* 2023;123:861-4.
104. Lee D, Swan CK, Suskind D, Wahbeh G, Vanamala J, Baldassano RN, et al. Children with Crohn's disease frequently consume select food additives. *Dig Dis Sci* 2018;63:2722-8.
105. Richey Levine A, Picoraro JA, Dorfzaun S, LeLeiko NS. Emulsifiers and intestinal health: an introduction. *J Pediatr Gastroenterol Nutr* 2022;74:314-9.
106. Martino JV, Van Limbergen J, Cahill LE. The role of carrageenan and carboxymethylcellulose in the development of intestinal inflammation. *Front Pediatr* 2017;5:96.